J. Fluid Mech. (1988), *vol.* 197, *pp.* 295–330
Printed in Great Britain

Nonlinear spatial evolution of an externally excited instability wave in a free shear layer

By M. E. GOLDSTEIN AND LENNART S. HULTGREN
National Aeronautics and Space Administration, Lewis Research Center,
Cleveland, OH 44135, USA

(Received 10 November 1987)

We consider a disturbance that evolves from a strictly linear finite-growth-rate instability wave, with nonlinear effects first becoming important in the critical layer. The local Reynolds number is assumed to be just small enough so that the spatial-evolution, nonlinear-convection, and viscous-diffusion terms are of the same order of magnitude in the interactive critical-layer vorticity equation. The numerical results show that viscous effects eventually become important even when the viscosity is very small due to continually decreasing scales generated by the nonlinear effects. The vorticity distribution diffuses into a more regular pattern vis-a-vis the inviscid case, and the instability-wave growth ultimately becomes algebraic. This leads to a new dominant balance between linear- and nonlinear-convection terms and an equilibrium critical layer of the Benney & Bergeron (1969) type begins to emerge, but the detailed flow field, which has variable vorticity within the cat's-eye boundary, turns out to be somewhat different from theirs. The solution to this rescaled problem is compared with the numerical results and is then used to infer the scaling for the next stage of evolution of the flow. The instability-wave growth is simultaneously affected by mean-flow divergence and nonlinear critical-layer effects in this latter stage of development and is eventually converted to decay. The neutral stability point is the same as in the corresponding linear case, however.

1. Introduction

Time-periodic excitation of (convectively unstable) free shear layers between parallel streams produces spatially growing instability waves that are initially governed by linear dynamics if the excitation amplitude is sufficiently small. While the amplitude continues to increase as the instability wave propagates downstream, its local growth rate must ultimately decrease owing to viscous spreading of the mean shear layer. Nonlinear effects can then become important in a critical layer at the transverse position where the phase velocity of the instability wave equals the mean velocity (once the instability-wave amplitude and growth rate become sufficiently large and small, respectively). The unsteady critical-layer motion is then governed by a nonlinear vorticity equation, while the flow outside the critical layer remains essentially linear.

The external instability-wave amplitude is completely controlled by the nonlinear dynamics of the critical layer, however. Goldstein & Leib (1988, hereinafter referred to as I) considered the case where the critical-layer vorticity equation represents a balance of spatial-evolution and (linear and nonlinear) convection terms. They show that this type of nonlinear critical layer occurs at the downstream position where the deviation of the local-thickness Strouhal number, or normalized frequency, from its

neutral value is $O(\epsilon^{\frac{1}{2}})$, where ϵ is the local instability-wave amplitude. The local Reynolds number R was assumed to be large enough so that viscous effects were unimportant in their analysis. The nonlinear effects then cause the instability wave to saturate well upstream of the linear neutral stability point, but with the final instability-wave amplitude oscillating about a finite non-zero value. It is unclear whether or not the 'outer' instability wave will reach a final equilibrium state. However, their numerical solutions clearly show that the critical-layer vorticity does not tend to a steady limit but continues to develop successively smaller lengthscales. Stewartson (1978) and Warn & Warn (1978) showed that spatially periodic Rossby-wave critical layers exhibit similar behaviour when they evolve in time. Stewartson (1978, 1981) concluded that even a very small viscosity would cause this latter type of critical layer to develop into an equilibrium critical layer of the Benney & Bergeron (1969) type, which has constant vorticity in the region of closed streamlines, the so-called Kelvin's cat's-eye.

A major purpose of the present investigation is to determine whether or not this hypothesis holds for spatially growing instability waves on shear layers between parallel streams by incorporating a small amount of viscosity into the analysis of I. The local Reynolds number R is here assumed to be just large enough so that the viscous-diffusion term is of the same order of magnitude as the spatial-evolution and nonlinear-convection terms in the critical-layer vorticity equation used in I. This corresponds to the Haberman (1972) scaling $R = O(\epsilon^{-\frac{3}{2}})$. The relative importance of viscous to nonlinear effects in the critical layer is then determined by the Haberman parameter, $\lambda = 1/\epsilon^{\frac{3}{2}}R$, while viscous effects play a purely passive role outside the critical layer.

Our analysis is related to that of Huerre & Scott (1980) but differs from it in at least one very important respect; namely, their critical layer is always an equilibrium critical layer (where the dominant balance is between linear-, i.e. mean-flow-, and nonlinear-convection effects) while ours is not. The important consequence is that Huerre & Scott's lowest-order instability-wave growth rate is much smaller than ours, $O(\epsilon^{\frac{3}{2}})$ as opposed to $O(\epsilon^{\frac{1}{2}})$, and is determined by the equilibrium (i.e. negligible growth rate) dynamics of Haberman (1972) rather than by non-equilibrium critical-layer dynamics as in the present investigation (where the dominant balance is between the growth-rate effects and the linear- and nonlinear-convection effects). It is also important to notice that Huerre & Scott (1980) had to impose an artificial body force to maintain parallel flow. This precludes the possibility of matching the solution onto the weakly non-parallel linear solution and, consequently, of imposing appropriate upstream boundary conditions, which is an important feature of the present analysis as well as that of I.

Our computations show the vorticity roll-up to be initially similar to the inviscid calculations of I, even when the scaled Haberman parameter (defined more precisely below) is ≈ 1, but viscous effects eventually assert themselves and cause the vorticity distribution to diffuse into a much simpler pattern (more characteristic of an equilibrium critical layer) once the nonlinear effects have had time to generate sufficiently small scales.

The instability-wave growth rate is always proportional to the phase jump across the critical layer; the latter being equal in the linear viscous and linear inviscid cases. Nonlinear effects drive the phase jump, and consequently the growth rate, toward zero (Gajjar & Smith 1985; Goldstein & Durbin 1986; Goldstein, Durbin & Leib 1987; Goldstein & Leib 1988). The present result shows that viscosity keeps the critical-layer phase jump from vanishing entirely and thereby has the rather

unexpected effect of allowing the instability wave to continue its growth asymptotically far downstream rather than saturating, as it appears to do in the inviscid case considered in I.

The resulting growth is admittedly very weak compared to the initial growth – being algebraic as opposed to exponential. This, however, still produces an unbounded increase of the nonlinear terms in the critical-layer vorticity equation so that a new dominant critical-layer balance between linear- and nonlinear-convection terms is eventually achieved. This is the situation that was analysed by Benney & Bergeron (1969). The lowest-order vorticity equation in this asymptotic region is equivalent to theirs, but it only determines the overall 'shell' of the solution. The detailed vorticity distribution is determined by a secularity condition and the transverse boundary conditions. The specific result turns out to be somewhat different from that of Benney & Bergeron (1969) and has variable vorticity in the closed-streamline region within the cat's-eye boundary. In this sense Stewartson's (1978, 1981) conjecture turns out to be incorrect for the present flow.

Benney & Bergeron (1969) invoked the Prandtl–Batchelor theorem (Batchelor 1956) to justify their assumption of constant cat's-eye vorticity. But this theorem assumes that the flow is no longer evolving or is evolving slowly enough from its initial state so that viscous effects have time to fully act on the motion – which is not the case in the present situation. Similar considerations may have led Stewartson (1981) to argue for constant vorticity from the fact that the variable-vorticity solution becomes logarithmically singular at the centre of the cat's-eye in the Benney–Bergeron scenario. Variable cat's-eye vorticity is an intrinsic attribute of the present solution, but the problem also possesses eigenfunctions that exhibit logarithmic singularities at the centre of the cat's-eye. However, the critical-layer vorticity equation has to be rescaled in this region (which brings back the viscous term) and the rescaled equation possesses a solution that remains bounded at the cat's-eye centre and matches (in the matched asymptotic expansion sense) onto any logarithmically singular solution that may exist outside this region. This means that the singular property cannot, in itself, be used to preclude the singular eigensolutions. However, a generalized Prandtl–Batchelor theorem, obtained from our non-equilibrium critical-layer vorticity equation, precludes the singular eigensolutions and yet allows variable cat's-eye vorticity.

The asymptotic weak algebraic growth of the instability wave allows the mean-flow divergence effects to alter the critical-layer structure before the instability wave achieves an $O(1)$ amplitude. The analytical solution of the rescaled problem for this next stage of evolution shows that the critical level moves across the shear (cf. Bodony, Smith & Gajjar 1983; Gajjar & Smith 1985) to maintain the quasi-equilibrium state against changes in mean flow. The resulting instability-wave growth is, therefore, simultaneously affected by mean-flow divergence and nonlinear critical-layer effects. The growth rate eventually goes to zero and the instability wave begins to decay. We show that the nonlinear effects have a strong influence on the maximum instability-wave amplitude but do not alter the location of the neutral stability point.

The problem is formulated in §2. where we show how the nonlinear critical layer gradually evolves from the strictly linear finite-growth-rate viscous solution and that there exists an overlap domain where these two solutions match (in the matched asymptotic expansion sense). We then indicate how the analysis of I can be modified to obtain the flow outside the critical layer. The critical-layer flow is analysed in §3. The vorticity satisfies a second-order partial differential equation in that region. This

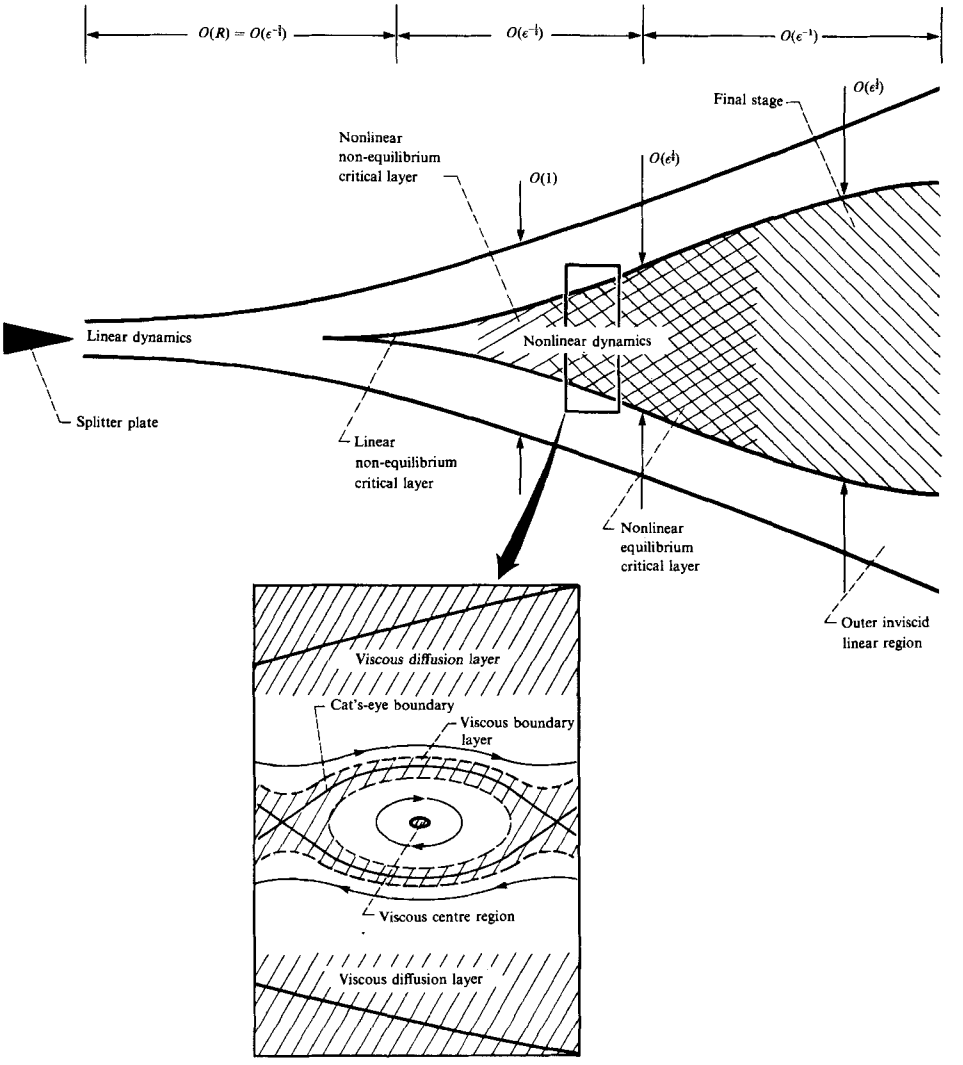

FIGURE 1. Flow structure.

equation is formally linear, but one of its coefficients depends on the unknown amplitude of the instability wave outside the critical layer. The overall problem is, therefore, nonlinear (and interactive) and has to be solved numerically. The numerical procedure is described in §4. An asymptotic solution to the critical-layer vorticity equation that applies at large downstream distances is constructed in §5. The numerical computations are discussed in §6 and a comparison is made with the asymptotic equilibrium critical-layer solution of the previous section. The relevant scaling and the solution for the next stage of evolution, where mean-flow divergence and nonlinear critical-layer effects both influence the evolution of the instability wave, are described in §7. The behaviour of the critical-layer vorticity at the cat's-eye centre is discussed in the Appendix. The flow structure is shown in figure 1.

2. Formulation and solution outside the critical layer

As in I, we are concerned with the two-dimensional flow of an incompressible and almost inviscid shear layer between two parallel streams with nominally uniform velocities $U_1 > U_2$. The streamwise and transverse coordinates (x and y), the time t, and all velocities are normalized by δ_0, δ_0/Δ, and Δ, respectively, where

$$\delta_0 = \tfrac{1}{2}\Theta_0, \tag{2.1}$$

Θ_0 is the momentum thickness of the unexcited shear layer at the origin of the x, y coordinates, and

$$\Delta = \tfrac{1}{2}(U_1 - U_2) \tag{2.2}$$

is a measure of the velocity difference across the shear layer.

We also assume that the mean-flow Reynolds number

$$R = \delta_0 \Delta/\nu, \tag{2.3}$$

where ν is the kinematic viscosity, is large enough and that the amplitude of the unsteady motion is small enough so that the mean flow is nearly parallel and the shear layer width – at least initially – increases only slowly over the long viscous scale

$$x_3 = x/R. \tag{2.4}$$

[Note the slight change of notation from I – x_2 will be introduced later as an intermediate scale.] As in I, the origin of the x, y coordinates is chosen so that the deviation,

$$\epsilon^{\frac{1}{2}} S_1 = S - S_0 < 0, \tag{2.5}$$

of the local Strouhal number S (the excitation angular frequency normalized by Δ/δ_0) from its neutral value S_0, as predicted by linear inviscid parallel flow stability theory, is $O(\epsilon^{\frac{1}{2}})$, where ϵ is a measure of the corresponding local instability-wave amplitude.

The shear-layer motion is again governed by the two-dimensional vorticity equation

$$\frac{\partial \omega}{\partial t} + \frac{\partial(\omega, \psi)}{\partial(\xi, y)} = \frac{1}{R}\nabla^2 \omega, \tag{2.6}$$

where

$$\omega = \nabla^2 \psi \tag{2.7}$$

is minus the dimensionless vorticity, and ψ is the stream function; ∇^2 is the Laplacian with respect to ξ and y,

$$\frac{\partial(\omega, \psi)}{\partial(\xi, y)} = \frac{\partial \omega}{\partial \xi}\frac{\partial \psi}{\partial y} - \frac{\partial \omega}{\partial y}\frac{\partial \psi}{\partial \xi}$$

is the Jacobian with respect to ξ and y of ω and ψ; and

$$\xi = x - \bar{U}t \tag{2.8}$$

denotes the streamwise coordinate in a reference frame moving with the normalized average velocity

$$\bar{U} = (U_1 + U_2)/2\Delta \tag{2.9}$$

of the two external streams.

The analysis of I shows that nonlinear critical-layer effects cause changes in the flow on the scale of the slow space and time variables

$$x_1 = \epsilon^{\frac{1}{2}} x \tag{2.10}$$

and

$$t_1 = \epsilon^{\frac{1}{2}} t. \tag{2.11}$$

This scaling remains unchanged even if we require that the Haberman (1972) parameter

$$\lambda = 1/\epsilon^{\frac{3}{2}} R \tag{2.12}$$

be $O(1)$ rather than imposing the more restrictive condition (2.11) of I, but viscous effects must now be accounted for in the analysis.

Since the (unexcited) basic-flow velocity U_{M} changes only on the slow viscous scale (2.4), it is sufficient to use its Taylor series expansion,

$$U_{\mathrm{M}} = U_0(y) + 2x_3 G'(y) + \ldots = U_0(y) + 2\epsilon\lambda x_1 G'(y) + O(\epsilon^2), \tag{2.13}$$

for the purpose of studying its changes on the nonlinear critical-layer streamwise lengthscale (2.10). Thus, we only require that the analysis be uniformly valid on the faster scale x_1 but not on the slower scale x_3. Variations on this latter scale are accounted for by the outer weakly non-parallel solution described in I (see figure 1). U_0 is determined by the imposed upstream profile and by the previous slow development of the mean flow on the long viscous scale $x_3 = x/R$. As in I, we assume that

$$U_0 = \bar{U} + \tanh y, \tag{2.14}$$

which closely corresponds to experimental observations and greatly simplifies the analysis. Then the neutral Strouhal number S_0 is again given by

$$S_0 = \bar{U}. \tag{2.15}$$

As explained in I, the slow variable t_1 will enter the solution only through

$$\zeta = \xi - S_1 t_1 = x - (\bar{U} + \epsilon^{\frac{1}{2}} S_1)\, t, \tag{2.16}$$

which denotes the streamwise coordinate in a reference frame moving with the actual phase velocity of the linear instability wave, and the solution outside the critical layer expands as

$$\psi = \psi_0(y) + \epsilon\psi_1 + \epsilon^{\frac{3}{2}}\psi_{\frac{3}{2}} + \epsilon^2\psi_2 + \epsilon^{\frac{5}{2}}\psi_{\frac{5}{2}} + O(\epsilon^3), \tag{2.17}$$

where the $\psi_{n/2}$ for $n \geqslant 2$ are functions of ζ and y and the slow variable x_1. ψ_0 is related to the zeroth-order term in the mean-flow Taylor-series expansion (2.13) by

$$U_0 = \bar{U} + \frac{\mathrm{d}\psi_0}{\mathrm{d}y}. \tag{2.18}$$

The first few $\psi_{n/2}$ are governed by

$$\mathscr{L}_0 \psi_1 = 0, \tag{2.19}$$

$$\mathscr{L}_0 \psi_{\frac{3}{2}} = -\mathscr{L}_1 \psi_1 + \lambda U''', \tag{2.20}$$

$$\mathscr{L}_0 \psi_2 = -\mathscr{L}_1 \psi_{\frac{3}{2}} - \Gamma_2 - \frac{\partial(\nabla^2\psi_1, \psi_1)}{\partial(\zeta, y)}, \tag{2.21}$$

$$\mathscr{L}_0\psi_{\frac{5}{2}} = -\mathscr{L}_1\psi_2 - \Gamma_{\frac{5}{2}} - \frac{\partial(\nabla^2\psi_1, \psi_{\frac{3}{2}})}{\partial(\zeta, y)} - \frac{\partial(\nabla^2\psi_{\frac{3}{2}} + 2\partial^2\psi_1/\partial\zeta\,\partial x_1, \psi_1)}{\partial(\zeta, y)} - \frac{\partial(\nabla^2\psi_1, \psi_1)}{\partial(x_1, y)} + \lambda\nabla^4\psi_1, \quad (2.22)$$

where

$$\mathscr{L}_0 = (U\nabla^2 - U'')\frac{\partial}{\partial\zeta}, \quad (2.23)$$

$$\mathscr{L}_1 = \left(-S_1\frac{\partial}{\partial\zeta} + U_0\frac{\partial}{\partial x_1}\right)\nabla^2 + \left(2U\frac{\partial^2}{\partial\zeta^2} - U''\right)\frac{\partial}{\partial x_1}, \quad (2.24)$$

$$\Gamma_2 = \left[(3U + 2\bar{U})\frac{\partial}{\partial x_1} - 2S_1\frac{\partial}{\partial\zeta}\right]\frac{\partial^2\psi_1}{\partial\zeta\,\partial x_1}, \quad (2.25)$$

$$\Gamma_{\frac{5}{2}} = \left[(3U + 2\bar{U})\frac{\partial}{\partial x_1} - 2S_1\frac{\partial}{\partial\zeta}\right]\frac{\partial^2\psi_{\frac{3}{2}}}{\partial\zeta\,\partial x_1} + \left(U_0\frac{\partial}{\partial x_1} - S_1\frac{\partial}{\partial\zeta}\right)\frac{\partial^2\psi_1}{\partial x_1^2}, \quad (2.26)$$

and $U = \tanh y$ have been introduced; ∇^2 now denotes the Laplacian with respect to ζ and y.

The first-order term ψ_1 is no longer just the linear instability wave solution as in I but is now the sum of the mean-flow change corresponding to the second term in (2.13) and the previous solution, i.e.

$$\psi_1 = \Phi_1^{(0)}(y, x_1) + \operatorname{sech} y\,\mathrm{Re}[A^\dagger(x_1)\,\mathrm{e}^{\mathrm{i}\zeta}], \quad (2.27)$$

The spatial growth of this wave is determined by the slowly varying amplitude function $A^\dagger$ which, along with the mean flow change $\Phi_1^{(0)}$, is ultimately determined by the second- and third-order problems.

Since the flow is still basically inviscid outside the critical layer, and since the phase jumps across the inviscid and viscous linear-growth critical layers are equal, $A\dagger$ must exhibit the same behaviour as $x_1 \to -\infty$ as in I, viz.

$$A^\dagger \to A_0^\dagger\,\mathrm{e}^{-\frac{1}{2}\kappa S_1 x_1} \quad \text{as} \quad x_1 \to -\infty, \quad (2.28)$$

where

$$\kappa = \kappa_r + \mathrm{i}\kappa_i = \frac{\pi}{1 + \frac{1}{2}\mathrm{i}\pi\bar{U}}. \quad (2.29)$$

The higher $\psi_{n/2}$ are of the form

$$\psi_{n/2} = \mathrm{Re}\left[\sum_{m=0}^{\infty}\Phi_{n/2}^{(m)}(y, x_1)\,\mathrm{e}^{\mathrm{i}m\zeta}\right] \quad \text{for} \quad n = 3, 4, \ldots, \quad (2.30)$$

with the formulas for $\Phi_{3/2}^{(m)}$ for $m = 0, 1, 2, \ldots$ and $\Phi_2^{(m)}$ for $m > 1$ being those of I, but the mean-flow term $\Phi_1^{(0)}$ now satisfies

$$\left(U_0\frac{\partial^2}{\partial y^2} - U_0''\right)\frac{\partial\Phi_1^{(0)}}{\partial x_1} = \lambda U_0'''. \quad (2.31)$$

It is sufficient to take (see 2.13), (2.17), and (2.27)

$$\Phi_1^{(0)} = \lambda x_1 U_0\left(\int_0^y \frac{U_0''}{U_0^2}\,\mathrm{d}y + 2c_1^{(0)}\right) = 2\lambda x_1 G(y), \quad (2.32)$$

where

$$G(y) = \tanh y - (\bar{U} + \tanh y)\left[\ln\frac{\bar{U} + \tanh y}{\bar{U}} - c_1^{(0)}\right], \quad (2.33)$$

and the constant $c_1^{(0)}$ is determined by the global mean-flow variation.

$\Phi_2^{(0)}$ is now determined by (3.29) of I with

$$\lambda^2 x_1^2 G'''(y) \tag{2.34}$$

added to the right-hand side. Since our interest here is primarily in the critical-layer flow we need only determine the contribution of (2.29) to the behaviour of $\Phi_1^{(0)}$ at the origin, i.e. $y = 0$. It clearly contributes a term of the form

$$\lambda^2 x_1^2 c_2^{(0)}, \tag{2.35}$$

where $c_2^{(0)}$ is a (possible zero) real constant. $\Phi_2^{(1)}$ is determined by (3.27) of I with

$$\left(\frac{\mathrm{d}^3 \Phi_1^{(0)}}{\mathrm{d}y^3} + 2\operatorname{sech}^2 y \frac{\mathrm{d}\Phi_1^{(0)}}{\mathrm{d}y}\right) A^\dagger \operatorname{cosech} y \tag{2.36}$$

added to the right-hand side. While $\Phi_2^{(1)}$ is now somewhat different from the $\Phi_2^{(1)}$ of I, it still behaves like (3.32) of I as $y \to 0$.

3. The critical layer

The analysis of the previous section was primarily carried out to determine the behaviour of the viscous outer solution in the neighbourhood of the critical layer (see figure 1). As in I, we introduce the scaled transverse coordinate

$$Y = y/\epsilon^{\frac{1}{2}} \tag{3.1}$$

into the solution (2.17) and re-expand with the inner variable Y held fixed.

The result is again given by (4.2) of I with the mean-flow correction

$$2\epsilon\lambda x_1 c_1^{(0)} \bar{U} + 2\epsilon^{\frac{3}{2}} \lambda x_1 c_1^{(0)} Y - \epsilon^2 (\lambda x_1 Y^2/\bar{U} - \lambda^2 x_1^2 c_2^{(0)}) \tag{3.2}$$

added to the right-hand side.

The critical-layer stream function ψ also here expands as

$$\Psi = \epsilon \Psi_0 + \epsilon^{\frac{3}{2}} \Psi_1 + \epsilon^2 \ln \epsilon^{\frac{1}{2}} \Psi_{2L} + \epsilon^2 \Psi_2 + \ldots, \tag{3.3}$$

where the Ψ_n are functions of ζ, Y, and x_1 only. Ψ_0 to Ψ_{2L} are given by (4.6) to (4.8) of I, but with $2\lambda x_1 c_1^{(0)} \bar{U}$ and $2\lambda x_1 c_1^{(0)} Y$ added to the right-hand sides of the first two equations, respectively. Ψ_2 is now determined by the viscous critical-layer vorticity equation

$$\mathscr{L}^{(I)} \Omega_1 = \lambda \Omega_{1_{YY}} \tag{3.4}$$

where, as in I,

$$\mathscr{L}^{(I)} = \bar{U} \frac{\partial}{\partial x_1} + (Y - S_1) \frac{\partial}{\partial \zeta} - \operatorname{Re}(iA^\dagger \mathrm{e}^{i\zeta}) \frac{\partial}{\partial Y}. \tag{3.5}$$

The $O(\epsilon)$ vorticity perturbation in the critical layer, $-\Omega_1$, is related to Ψ_2 through

$$\Psi_{2_{YY}} = \Omega_1 - \Psi_{0_{\zeta\zeta}} = \Omega_1 + \operatorname{Re}(A^\dagger \mathrm{e}^{-i\zeta}). \tag{3.6}$$

and the total critical-layer vorticity is given by $-(1 + \epsilon\Omega_1) + O(\epsilon^{\frac{3}{2}})$.

In the present case, it is convenient to define $Q^\dagger$ by

$$\Omega_1 = -Y^2 - 2\lambda x_1/\bar{U} - 2\operatorname{Re}(A^\dagger \mathrm{e}^{i\zeta}) + Q^\dagger \tag{3.7}$$

rather than by (4.17) of I. Consideration of the dominant balance as $|Y| \to \infty$ of (3.4), with (3.7), shows that $Q^\dagger$ still has the asymptotic behaviour given by (4.22) of I. The error term R_0 is still $O(Y^{-3})$, but, of course, is no longer given by (4.23) of I.

Integration of (3.6) with respect to Y from $-M$ to M, letting $M \to \infty$, and using the inner limit of the outer solution again produces the matching condition (4.25) of I. By then, using (3.20) of I, it follows that $Q^\dagger$ as before satisfies the jump condition

$$\int_0^{2\pi} \int_{-\infty}^{+\infty} e^{-i\zeta} Q^\dagger \, d\zeta \, dY = 4\pi i \frac{dA^\dagger}{dx_1}. \tag{3.8}$$

Moreover, it is again convenient to introduce the rescaled variables (4.26)–(4.32) of I, i.e.

$$Q = Q^\dagger / S_1^2 \bar{U}, \tag{3.9}$$

$$A = 4A^\dagger e^{iX_0} / S_1^2 \bar{U}^2, \tag{3.10}$$

$$\eta = -2(Y - S_1)/S_1 \bar{U}, \tag{3.11}$$

$$X = \zeta - X_0, \tag{3.12}$$

$$\bar{x} = -S_1 x_1/2 - x_0, \tag{3.13}$$

$$x_0 = \frac{1}{\kappa_r} \ln \frac{(S_1 \bar{U})^2}{4|A_0^\dagger|}, \tag{3.14}$$

$$X_0 = -\kappa_i x_0 - \arg A_0^\dagger. \tag{3.15}$$

Then it follows from (2.28), (2.29), and (3.4)–(3.8) that Q and A satisfy the scaled critical-layer vorticity equation

$$\left[\frac{\partial}{\partial \bar{x}} + \eta \frac{\partial}{\partial X} - \mathrm{Re}\,(iA\, e^{iX}) \frac{\partial}{\partial \eta} - \bar{\lambda} \frac{\partial^2}{\partial \eta^2}\right] Q = \mathrm{Re}\left[\left(\frac{\bar{U}}{2} \frac{dA}{d\bar{x}} + iA\right) e^{iX}\right], \tag{3.16}$$

subject to the upstream boundary condition

$$A \to e^{\kappa \bar{x}} \quad \text{as} \quad \bar{x} \to -\infty \tag{3.17}$$

along with the transverse boundary condition

$$Q \to 0 \quad \text{as} \quad |\eta| \to \infty \tag{3.18}$$

and the transverse jump condition

$$\frac{1}{\pi} \int_0^{2\pi} \int_{-\infty}^{+\infty} e^{-iX} Q \, dX \, d\eta = i \frac{dA}{d\bar{x}}, \tag{3.19}$$

where we have put

$$\bar{\lambda} = 8\lambda/(-S_1 \bar{U})^3. \tag{3.20}$$

It follows from (2.29) and (3.17) that the third (i.e. the nonlinear) term on the left-side of (3.16) drops out as $\bar{x} \to -\infty$ and, consequently, that

$$Q \to \mathrm{Re}\,[\kappa(i/\bar{\lambda})^{\frac{1}{3}} q(z)\, e^{\kappa \bar{x} + iX}] \quad \text{as} \quad \bar{x} \to -\infty, \tag{3.21}$$

where

$$z = (i/\bar{\lambda})^{\frac{1}{3}} (\eta - i\kappa), \tag{3.22}$$

and q satisfies the inhomogeneous Airy's equation

$$\frac{d^2 q}{dz^2} - zq = -\frac{1}{\pi}, \tag{3.23}$$

subject to the integral constraint

$$\int_{-\infty}^{+\infty} q \, dz = i. \tag{3.24}$$

Equations (3.23) and (3.24) have the solution

$$q = \mathrm{Gi}(z) + \mathrm{i}\,\mathrm{Ai}(z), \tag{3.25}$$

where Gi is the particular solution of (3.23) defined on p. 448 of Abramowitz & Stegun (1964). This is the usual solution for the vorticity in the linear viscous-growth critical layer.

$$\int_0^{2\pi}\int_{-\infty}^{+\infty} Q\,\mathrm{d}X\,\mathrm{d}\eta = 0 \tag{3.26}$$

must also be satisfied in the present situation, which we show to be the case in the next section.

4. Numerical computation

The nonlinear evolution equations (3.15)–(3.20) must, of course, be solved by numerical methods. Since Q is periodic in X, it can be expanded in a Fourier series

$$Q = \frac{1}{2}\sum_{n=-\infty}^{\infty} Q_n(\bar{x},\eta)\,\mathrm{e}^{\mathrm{i}nX}, \quad Q_{-n} = Q_n^*, \tag{4.1}$$

where the asterisk denotes the complex conjugate. Substitution of (4.1) into the evolution equations (3.16)–(3.21) leads to

$$\left(\frac{\partial}{\partial\bar{x}} + \mathrm{i}n\eta\right)Q_n + \frac{\mathrm{i}}{2}\frac{\partial}{\partial\eta}\left(A^*Q_{n+1} - AQ_{n-1}\right) - \bar{\lambda}\frac{\partial^2 Q_n}{\partial\eta^2} = \delta_{n1}\left(\frac{\bar{U}}{2}\frac{\mathrm{d}A}{\mathrm{d}x} + \mathrm{i}A\right), \tag{4.2}$$

for $n \geqslant 0$, where δ_{ij} is the Kronecker delta tensor, and

$$\int_{-\infty}^{\infty} Q_1\,\mathrm{d}\eta = \mathrm{i}\frac{\mathrm{d}A}{\mathrm{d}\bar{x}}, \tag{4.3}$$

with the upstream conditions (3.17) and

$$Q_n \to \delta_{n1}\kappa(\mathrm{i}/\bar{\lambda})^{\frac{1}{3}}q(z)\,A \quad \text{as} \quad \bar{x}\to-\infty. \tag{4.4}$$

Equations (4.22) of I, (3.9)–(3.12), (4.1) and (4.2) show that as $\eta\to\infty$

$$Q_0 \to \frac{\bar{U}}{4\eta^2}|A|^2 + O(\eta^{-3}), \tag{4.5}$$

$$Q_1 \to -\frac{\mathrm{i}}{\eta}\left(\frac{\bar{U}}{2}\frac{\mathrm{d}A}{\mathrm{d}\bar{x}} + \mathrm{i}A\right) + \frac{1}{\eta^2}\left(\frac{\bar{U}}{2}\frac{\mathrm{d}^2A}{\mathrm{d}\bar{x}^2} + \mathrm{i}\frac{\mathrm{d}A}{\mathrm{d}x}\right) + O(\eta^{-3}), \tag{4.6}$$

$$Q_n \to O(\eta^{-n-1}), \quad n \geqslant 2. \tag{4.7}$$

Integration of (4.2) with $n = 0$ and using (4.6) shows that

$$\frac{\mathrm{d}}{\mathrm{d}\bar{x}}\int_{-\infty}^{\infty} Q_0\,\mathrm{d}\eta = 0. \tag{4.8}$$

Since $Q_0\to 0$ as $\bar{x}\to-\infty$ this implies that

$$\int_{-\infty}^{\infty} Q_0\,\mathrm{d}\eta = 0 \tag{4.9}$$

and, consequently, that (3.26) is indeed satisfied.

Rather than mapping the infinite domain $-\infty < \eta < +\infty$ into a finite region, equation (4.2) is solved over a finite range, say $-M < \eta < M$, and the asymptotic behaviour of Q, (4.5)–(4.7), is used to set the boundary conditions. The integral over the infinite domain in (4.3) is approximated using a technique analogous to the one developed by Haynes (1985). The resulting formula for $\mathrm{d}A/\mathrm{d}\bar{x}$, involving only integrals over a finite interval, reads

$$\left[1+2\bar{U}^2-\frac{4}{M}\left(1-\frac{1}{M}\right)\right]\frac{\mathrm{d}A}{\mathrm{d}x} = -2\mathrm{i}\bar{U}A-\mathrm{i}\left(1-\frac{2}{M}+\bar{U}^2\right)I_{10}+\mathrm{i}\frac{\bar{U}}{M}I_{11} -\mathrm{i}\left(\frac{\bar{U}}{M}\right)^2(I_{12}-\tfrac{1}{2}A^*I_{20})+O(M^{-3}), \quad (4.10)$$

where

$$I_{nm} = \int_{-M}^{M} Q_n \eta^m \,\mathrm{d}\eta. \quad (4.11)$$

The η-derivatives in (4.2) were discretized using central-difference approximations and Simpsons' rule was used for the integrals in (4.10). The solution of (4.10) and (4.2) was marched forward in $\bar{x}$ through a predictor–corrector procedure. A third-order scheme was used for (4.10). The predictor step for (4.2) consisted of a second-order Adams–Bashforth approximation for the nonlinear and inhomogeneous terms and the Crank–Nicholson (second-order implicit) approximation for the mean-flow convection and the viscous terms. The corrector step was fully of the Crank–Nicholson type. Thomas' algorithm was used to solve the resulting finite-difference approximation of (4.2) in both steps. The combined corrector steps for (4.10) and (4.2) was then iterated until the solution at the next streamwise station had been obtained to within a preset tolerance.

5. The limiting form of the critical-layer vorticity

In this section, we derive an asymptotic solution to the boundary-value problem (3.16)–(3.19) that is valid in the limit as the slow streamwise variable $\bar{x}$ becomes infinite. The numerical results, which are discussed much more fully in §6 below, show that, no matter how small the viscous parameter $\bar{\lambda}$, the amplitude A eventually exhibits algebraic growth as $\bar{\lambda}\bar{x}$ becomes large. This produces an increase in the critical-layer width on the order of $a^{\frac{1}{2}}$ and a transverse shift in its location by an amount $\Theta' = \mathrm{d}\Theta/\mathrm{d}x$, where $a = |A|$ and the phase Θ is defined by

$$A = a\,\mathrm{e}^{-\mathrm{i}\Theta}. \quad (5.1)$$

That, in turn, suggests the introduction of the new rescaled variables

$$\bar{X} = X-\Theta(\bar{x}), \quad (5.2)$$

$$\bar{\eta} = (\eta-\Theta')/a^{\frac{1}{2}}, \quad (5.3)$$

$$\bar{Q} = Q/a^{\frac{1}{2}} \quad (5.4)$$

into (3.16), (3.19), and (3.26). The polar form (5.1) for the complex amplitude A and the shifted streamwise variable $\bar{X}$ are used to simplify the analysis. The transformation (5.3) ensures that the shifted and rescaled transverse coordinate $\bar{\eta}$ remains centred within the critical layer and continues to scale with the critical-layer width. Finally, the scaling (5.4) is chosen so that the dominant inhomogeneous term

appears in the lowest-order equation. The rescaled nonlinear evolution equations become

$$\bar{\eta}\frac{\partial \bar{Q}}{\partial \bar{X}}+\sin\bar{X}\frac{\partial \bar{Q}}{\partial \bar{\eta}}=\left(\frac{\bar{U}}{2}\Theta'-1\right)\sin\bar{X}+\frac{\bar{U}a'}{2a}\cos\bar{X}+\frac{\bar{\lambda}}{a^{\frac{3}{2}}}\frac{\partial^2\bar{Q}}{\partial\bar{\eta}^2}$$
$$+\frac{\Theta''}{a}\frac{\partial\bar{Q}}{\partial\bar{\eta}}-\frac{1}{a^{\frac{1}{2}}}\left[\frac{\partial\bar{Q}}{\partial\bar{x}}+\frac{a'}{2a}\left(\bar{Q}-\bar{\eta}\frac{\partial\bar{Q}}{\partial\bar{\eta}}\right)\right], \quad (5.5)$$

$$\frac{1}{\pi}\int_0^{2\pi}\int_{-\infty}^{+\infty}\mathrm{e}^{-\mathrm{i}\bar{X}}\,\bar{Q}\,\mathrm{d}\bar{X}\,\mathrm{d}\bar{\eta}=\Theta'+\mathrm{i}\frac{a'}{a}, \quad (5.6)$$

$$\int_0^{2\pi}\int_{-\infty}^{+\infty}\bar{Q}\,\mathrm{d}\bar{X}\,\mathrm{d}\bar{\eta}=0, \quad (5.7)$$

where the prime now denotes differentiation with respect to $\bar{x}$. The two terms on the right-hand side of (5.6) correspond to the velocity jump and the phase jump across the critical layer, respectively; and (5.7) is the mean-flow jump condition.

The left-hand side of (5.5) is the convective derivative of $\bar{Q}$ along the 'zeroth-order streamlines' $\bar{\phi}=$ constant, where

$$\bar{\phi}=\bar{\eta}^2+2\cos\bar{X}. \quad (5.8)$$

These streamlines have the familiar Kelvin's cat's-eye pattern with closed streamlines inside the cat's-eye boundary $\bar{\phi}=2$ and open streamlines outside.

The overall structure of the asymptotic solution is rather complicated but many of its features have already been considered by Benney & Bergeron (1969), Brown & Stewartson (1978), Smith & Bodonyi (1982), and others in the context of equilibrium critical layers. The present problem is, however, sufficiently different to require that a detailed description of the solution procedure be given. To ease the burden on the reader we begin with an overall summary of the various steps involved in the analysis. The exact (i.e. the numerical) solution to the original boundary-value problem (3.16)–(3.19) (or, equivalently, to the rescaled problem (5.5)–(5.7)) is not only continuous but has continuous derivatives to all orders everywhere in the flow. It is, on the other hand, possible to construct asymptotic solutions that violate these requirements to some degree. The continuity requirement can manifest itself as solvability conditions for higher-order problems in the expansion in ways that are not always easy to sort out and which can, in any event, introduce considerable complexity into the analysis. These complications can be minimized by using the unexpanded vorticity equation (5.5) to derive an additional integral constraint, which the exact solution will automatically satisfy, but which can be imposed (as an additional restriction) on the asymptotic solution to ensure that its higher-order terms exhibit proper behaviour. This is done in §5.1 below.

Much of the complexity of the present analysis is due to the multilayered structure of the asymptotic solution (see figure 1). The flow is predominantly inviscid in the main layer, where $\bar{\eta}=O(1)$, and exhibits different behaviour inside and outside the cat's eye. The relevant solution is constructed in §5.2, where the integral constraint of §5.1 is used to further restrict its form. The result does not satisfy the outer (large-$\bar{\eta}$) boundary condition and an adjustment has to take place through an outer diffusive layer. The relevant scaling for this outer region is described in §5.3 and an appropriate asymptotic solution is constructed.

The inner and outer expansions are matched in §5.4 and an appropriate uniformly valid composite solution is then constructed. This is done to facilitate the imposition

of the integral constraints (5.6) and (5.7). Section 5.5 considers the mean-flow constraint (5.7) and the velocity-jump constraint, the latter being the real part of (5.6). The phase-jump constraint, i.e. the imaginary part of (5.6), involves a contribution from a viscous boundary layer (or internal shear layer) that forms on the cat's-eye boundary to smooth out a discontinuity in the derivative of the inviscid solution of §5.2 across that boundary. The boundary-layer solution is briefly described in §5.6 and the phase-jump constraint is then imposed.

These constraints uniquely determine the coefficients in the asymptotic expansion for the amplitude a and phase Θ and explicit formulas are given in §5.7. The analysis can be carried to higher order and we give the next-order terms in the expansion for these quantities, but without showing the actual derivation.

5.1. *The generalized Prandtl–Batchelor theorem*

Equation (5.5) is equivalent to the two first-order equations

$$\frac{\partial \bar{H}}{\partial \bar{X}} + \sin \bar{X} \bar{Q} = \bar{\eta}\left[\left(\frac{\bar{U}}{2}\Theta' - 1\right)\sin \bar{X} + \frac{\bar{U}a'}{2a}\cos \bar{X}\right] + \frac{\bar{\lambda}}{a^{\frac{3}{2}}}\frac{\partial \bar{Q}}{\partial \bar{\eta}} + \left(\frac{\Theta''}{a} + \frac{a'\bar{\eta}}{2a^{\frac{3}{2}}}\right)\bar{Q} - \frac{1}{a^{\frac{1}{2}}}\left(\frac{\partial}{\partial \bar{x}} + \frac{a'}{a}\right)\int^{\bar{\eta}} \bar{Q}\, \mathrm{d}\bar{\eta}, \quad (5.9)$$

$$\frac{\partial \bar{H}}{\partial \bar{\eta}} - \bar{\eta}\bar{Q} = 0, \quad (5.10)$$

where $\bar{H}$ is a single-valued function of $\bar{X}$, $\bar{\eta}$, and $\bar{x}$.

Since the integral around a closed streamline, $\bar{\phi}$ = constant, of the left-hand side of the result of adding $[(\mathrm{d}\bar{\eta}/\mathrm{d}\bar{X})_{\bar{\phi}}^2 + 1]^{-\frac{1}{2}}$ times the first equation to $[(\mathrm{d}\bar{X}/\mathrm{d}\bar{\eta})_{\bar{\phi}}^2 + 1]^{-\frac{1}{2}}$ times the second is identically zero, the integral on the right-hand side must also vanish and it follows that

$$\oint\left[\frac{\bar{U}a'}{2a}\bar{\eta}\cos \bar{X} + \frac{\bar{\lambda}}{a^{\frac{3}{2}}}\frac{\partial \bar{Q}}{\partial \bar{\eta}} + \left(\frac{\Theta''}{a} + \frac{a'\bar{\eta}}{2a^{\frac{3}{2}}}\right)\bar{Q} - \frac{1}{a^{\frac{1}{2}}}\left(\frac{\partial}{\partial \bar{x}} + \frac{a'}{a}\right)\int^{\bar{\eta}} \bar{Q}\, \mathrm{d}\bar{\eta}\right]\mathrm{d}\bar{X} = 0, \quad (5.11)$$

where $\oint$ denotes an integral around a closed streamline.

This result can also be obtained by applying the Stokes' integral theorem to the integral of (5.5) over the interior of a typical closed streamline. We refer to it as the generalized Prandtl–Batchelor theorem, since we shall use it to determine the vorticity in the closed-streamline region.

5.2. *Asymptotic solution in the central region* $\bar{\eta} = O(1)$

We shall seek an asymptotic solution, valid as $\bar{\lambda}\bar{x} \to \infty$, by expanding a, Θ', and $\bar{Q}$ in powers (and logarithms) of $\bar{\lambda}\bar{x}$. The numerical results (see §6 below) suggest that $a \sim (\bar{\lambda}\bar{x})^{\gamma}$, with $0 < \gamma \leqslant \frac{2}{3}$, and $\Theta' \sim$ constant as $\bar{\lambda}\bar{x} \to \infty$. The lowest-order solution imposes no specific restriction on γ and the dominant asymptotic form of Θ'. However, the relevant higher-order solutions can only satisfy the imaginary part of the integral constraints (5.6) (i.e. the phase-jump condition) if $\Theta' \sim \bar{x}^{3\gamma/2-1}$ as $\bar{x} \to \infty$. Then, the lowest-order solution cannot satisfy the other integral constraints, i.e. the real part of (5.6), (5.7), and (5.11), unless $\gamma = \frac{2}{3}$. This is best demonstrated by carrying out the solution with γ and Θ' unrestricted. But that would greatly complicate the presentation since several different expansion forms would then have to be considered. To avoid this complexity, we set $\gamma = \frac{2}{3}$ at the outset, assume, as the

numerical solution suggests, that Θ' is constant to leading order, and rely on the internal consistency of the resulting expansions and its good agreement with the numerical solution to justify our choice. We, therefore, seek a solution of the form

$$a = a_\infty(\bar\lambda\bar x)^{\frac{2}{3}}[1+a_1(\bar\lambda\bar x)^{-\frac{1}{6}}+a_2(\bar\lambda\bar x)^{-\frac{1}{3}}+\ldots+a_6(\bar\lambda\bar x)^{-1}+\ldots], \tag{5.12}$$

$$\Theta' = \theta'_\infty[1+\theta_1(\bar\lambda\bar x)^{-\frac{1}{6}}+\theta_2(\bar\lambda\bar x)^{-\frac{1}{3}}+\ldots+\theta_6(\bar\lambda\bar x)^{-1}+\ldots], \tag{5.13}$$

$$\bar Q = [b_{0L}+b_{1L}(\bar\lambda\bar x)^{-\frac{1}{6}}+b_{2L}(\bar\lambda\bar x)^{-\frac{1}{3}}+\ldots+b_{6L}(\bar\lambda\bar x)^{-1}+\ldots]\ln\left(\frac{a_\infty}{(\bar\lambda\bar x)^{\frac{1}{3}}}\right)$$
$$+Q^{(0)}+(\bar\lambda\bar x)^{-\frac{1}{6}}Q^{(1)}+(\bar\lambda\bar x)^{-\frac{1}{3}}Q^{(2)}+\ldots+(\bar\lambda\bar x)^{-1}Q^{(6)}+\ldots, \tag{5.14}$$

where a_∞, a_1, $a_2,\ldots$, θ'_∞, θ_1, $\theta_2,\ldots$, and b_{0L}, b_{1L}, $b_{2L},\ldots$ are constants and the $Q^{(n)}$ depend on $\bar X$ and $\bar\eta$. The term involving the logarithm was introduced to facilitate matching with an outer diffusion solution to be discussed below.

Then $Q^{(0)}$ to $Q^{(5)}$ satisfy

$$\left(\bar\eta\frac{\partial}{\partial\bar X}+\sin\bar X\frac{\partial}{\partial\bar\eta}\right)Q^{(n)} = \operatorname{sgn}\bar\eta\,(\bar\phi-2\cos\bar X)^{\frac{1}{2}}\frac{\partial Q^{(n)}}{\partial\bar X} = e_n\sin X \quad \text{for } n=0,\,1,\ldots,\,5, \tag{5.15}$$

where $\bar\phi$ is defined by (5.8), the partial derivative with respect to $\bar X$ is at constant $\bar\phi$ in the second member (but not the first), and we have put

$$e_0 = \frac{\bar U}{2}\theta'_\infty - 1, \tag{5.16}$$

$$e_n = \frac{\bar U}{2}\theta'_\infty\theta_n, \quad n>0. \tag{5.17}$$

Equations (5.15)–(5.17) imply that

$$Q^{(n)} = F^{(n)}(\bar\phi)+e_n\bar\eta, \quad n=0,\,1,\,2,\ldots,5, \tag{5.18}$$

where, except for the requirement

$$F^{(0)}\to-\operatorname{sgn}\bar\eta\,e_0\bar\phi^{\frac{1}{2}} \quad \text{as} \quad \bar\phi\to\infty \tag{5.19}$$

imposed by (3.18), $F^{(0)}$ to $F^{(5)}$ are, at this stage, arbitrary functions of their argument. $Q^{(0)}$ is of the same form as the lowest-order solution obtained by Benney & Bergeron (1969) for the inviscid equilibrium critical layer.

The intermediate terms in the expansion $Q^{(1)}$ to $Q^{(5)}$ play no essential role in the determination of $F^{(0)}$, but $Q^{(6)}$ does. The latter quantity is determined by

$$\left(\bar\eta\frac{\partial}{\partial\bar X}+\sin\bar X\frac{\partial}{\partial\bar\eta}\right)Q^{(6)} = e_6\sin\bar X+\bar\lambda\left(\frac{\bar U}{3}\cos\bar X+\frac{1}{a_\infty^{\frac{3}{2}}}\frac{\partial^2F^{(0)}}{\partial\bar\eta^2}\right) \tag{5.20}$$

and must satisfy certain periodicity and continuity requirements. Since the left-hand side of (5.20) is equal to $\bar\eta(\partial Q^{(6)}/\partial\bar X)_{\bar\phi}$ and $\partial/\partial\bar\eta = 2\bar\eta\partial/\partial\bar\phi$, this equation can be integrated immediately with respect to $\bar X$ to obtain

$$Q^{(6)} = \frac{4\bar\lambda}{a_\infty^{\frac{3}{2}}}\frac{\partial}{\partial\bar\phi}\left(F^{(0)\prime}\int_\beta^{\bar X}\bar\eta\,\mathrm{d}\bar X+\alpha_\infty\int_\beta^{\bar X}\bar\eta\cos\bar X\,\mathrm{d}\bar X\right)+e_6\bar\eta+F^{(6)}(\bar\phi), \tag{5.21}$$

where
$$\alpha_\infty = \frac{\bar{U} a_\infty^{\frac{3}{2}}}{6}, \tag{5.22}$$

$$\beta = \begin{cases} 0, & \bar{\phi} > 2 \\ \cos^{-1}\dfrac{\bar{\phi}}{2}, & -2 \leqslant \bar{\phi} < 2. \end{cases} \tag{5.23}$$

The first term on the right-hand side of (5.21) corresponds to the viscous correction obtained by Benney & Bergeron (1969). Unlike $Q^{(0)}$ to $Q^{(5)}$, the solution (5.21) for $Q^{(6)}$ is not periodic outside the cat's eye and is, in general, discontinuous across $\bar{\eta} = 0$ inside the cat' eye. It can be made periodic and continuous by requiring that $F^{(0)}$ satisfy

$$(IF^{(0)\prime} + \alpha_\infty I_1)' = 0, \tag{5.24}$$

where
$$I(\bar{\phi}) = \int_\beta^{2\pi-\beta} (\phi - 2\cos\bar{X})^{\frac{1}{2}} \mathrm{d}\bar{X}, \tag{5.25}$$

$$I_1(\bar{\phi}) = \int_\beta^{2\pi-\beta} (\bar{\phi} - 2\cos\bar{X})^{\frac{1}{2}} \cos\bar{X}\, \mathrm{d}\bar{X}. \tag{5.26}$$

Since
$$I \sim 2\pi\bar{\phi}^{\frac{1}{2}}\left[1 - \frac{1}{4\bar{\phi}^2} + O(\bar{\phi}^{-4})\right], \tag{5.27}$$

$$I_1 \sim -\frac{\pi}{\bar{\phi}^{\frac{1}{2}}}\left[1 + \frac{3}{8\bar{\phi}^2} + O(\bar{\phi}^{-4})\right], \tag{5.28}$$

as $\bar{\phi} \to \infty$, the solution to (5.24) that satisfies (5.19) and is continuous across $\bar{\phi} = 2$ is given by

$$F^{(0)}(\bar{\phi}) = b_0 \mp \pi e_0 \int_2^{\bar{\phi}} \frac{\mathrm{d}\bar{\phi}}{I} - \alpha_\infty \int_2^{\bar{\phi}} \frac{I_1}{I}\mathrm{d}\bar{\phi}, \quad \bar{\phi} > 2, \quad \bar{\eta} \gtrless 0, \tag{5.29}$$

$$F^{(0)}(\bar{\phi}) = b_0 + c_0 \int_2^{\bar{\phi}} \frac{\mathrm{d}\bar{\phi}}{I} - \alpha_\infty \int_2^{\bar{\phi}} \frac{I_1}{I}\mathrm{d}\bar{\phi}, \quad \bar{\phi} < 2. \tag{5.30}$$

Inserting the expansions (5.12)–(5.14) into the generalized Prandtl–Batchelor constrant (5.11), equating coefficients of $(\bar{\lambda}\bar{x})^{-1}$, and using (5.18), (5.25), and (5.26) leads to

$$IF^{(0)\prime} + \alpha_\infty I_1 = 0 \quad \text{for} \quad -2 < \bar{\phi} < 2. \tag{5.31}$$

Inserting (5.30) into (5.31) shows that

$$c_0 = 0. \tag{5.32}$$

The coefficient of c_0 in (5.30) has a logarithmic singularity at the centre of the cat's eye. Stewartson (1981) argued for constant cat's-eye vorticity in the Benney–Bergeron solution by pointing out that the variable-vorticity solution has a similar singularity in that case. However, the Appendix shows that this singularity can be eliminated and therefore that the singular behaviour alone cannot be used to preclude such solution, which is, of course, why the present approach had to be used.

5.3. *The outer diffusion layer*

While the requirement (5.19) is necessary to ensure that Q satisfy the original boundary condition (3.18), it is certainly not sufficient. In fact, (5.4), (5.14), (5.18), and (5.27)–(5.29) show that Q does *not* satisfy this condition, so that $Q^{(0)}$ has to be

brought to zero through an outer diffusion layer, as suggested by Stewartson (1981) (see figure 1). The appropriate scaled cross-stream variable in that region is

$$\hat{\eta} = (\eta - \Theta')/(\bar{l}\bar{x})^{\frac{1}{2}}. \tag{5.33}$$

Introducing this variable along with (5.1), (5.2), and (5.4) in (3.16) yields

$$\hat{\eta}\frac{\partial \bar{Q}}{\partial \bar{X}} = \left(\frac{a}{\bar{\lambda}\bar{x}}\right)^{\frac{1}{2}}\left[\left(\frac{\bar{U}}{2}\Theta' - 1\right)\sin\bar{X} + \frac{\bar{U}a'}{2a}\cos\bar{X}\right] - \frac{a}{\bar{\lambda}\bar{x}}\left(\sin\bar{X} - \frac{\Theta''}{a}\right)\frac{\partial \bar{Q}}{\partial \hat{\eta}} + \frac{\bar{\lambda}}{(\bar{\lambda}\bar{x})^{\frac{3}{2}}}\left(\frac{\partial^2 \bar{Q}}{\partial \hat{\eta}^2} + \frac{\hat{\eta}}{2}\frac{\partial \bar{Q}}{\partial \hat{\eta}} - \frac{\bar{x}a'}{2a}\bar{Q} - \bar{x}\frac{\partial \bar{Q}}{\partial \bar{x}}\right). \tag{5.34}$$

When $\hat{\eta} = O(1)$, the solution to this equation expands like

$$\bar{Q} = \hat{F}(\bar{\lambda}\bar{x}, \hat{\eta}) - \left(\frac{a}{\bar{\lambda}\bar{x}}\right)^{\frac{1}{2}}\frac{1}{\hat{\eta}}\left[\left(\frac{\bar{U}}{2}\Theta' - 1\right)\cos\bar{X} - \frac{\bar{U}a'}{2a}\sin\bar{X}\right] + \frac{a}{\bar{\lambda}\bar{x}}\frac{1}{\hat{\eta}}\frac{\partial \hat{F}}{\partial \hat{\eta}}\cos\bar{X} + \frac{1}{4}\left(\frac{a}{\bar{\lambda}\bar{x}}\right)^{\frac{3}{2}}\frac{1}{\hat{\eta}^3}\left[\left(\frac{\bar{U}}{2}\Theta' - 1\right)\cos 2\bar{X} - \frac{\bar{U}a'}{2a}\sin 2\bar{X}\right] + \ldots, \tag{5.35}$$

$$\hat{F} = \hat{F}^{(0)}(\hat{\eta}) + (\bar{\lambda}\bar{x})^{-\frac{1}{6}}\hat{F}^{(1)}(\hat{\eta}) + \ldots, \tag{5.36}$$

as $\bar{\lambda}\bar{x} \to \infty$; $\hat{F}^{(0)}$ is determined by the solvability condition for the $O[(\bar{\lambda}\bar{x})^{-\frac{3}{2}}]$ problem

$$\hat{F}^{(0)\prime\prime} + \frac{\hat{\eta}}{2}\hat{F}^{(0)\prime} - \frac{1}{3}\hat{F}^{(0)} = -\frac{\alpha_\infty}{\hat{\eta}^2}, \tag{5.37}$$

where the prime denotes differentiation with respect to the argument. This condition follows from the requirement that the $\bar{X}$-independent inhomogeneous terms cancel at that order.

Equation (5.37) transforms into Kummer's equation upon introducing the new independent variable

$$\hat{\phi} = \tfrac{1}{4}\hat{\eta}^2. \tag{5.38}$$

The solution that vanishes as $\hat{\phi} \to \infty$ is, then, given by

$$\hat{F}^{(0)} = \alpha_\infty \hat{F}_{\mathrm{p}} + \hat{b}^{(0)}_{\gtrless}\, \mathrm{e}^{-\hat{\phi}}\, U(\tfrac{5}{6}, \tfrac{1}{2}, \hat{\phi}), \tag{5.39}$$

where the $\hat{F}_{\mathrm{p}}$ denotes the particular solution

$$\hat{F}_{\mathrm{p}} = \frac{\Gamma(\frac{5}{6})}{4\pi^{\frac{1}{2}}}\mathrm{e}^{-\hat{\phi}}\left\{U(\tfrac{5}{6}, \tfrac{1}{2}, \hat{\phi})\left[\int_0^{\hat{\phi}}\left(M(\tfrac{5}{6}, \tfrac{1}{2}, t) - 1\right)\frac{\mathrm{d}t}{t^{\frac{3}{2}}} - \frac{2}{\hat{\phi}^{\frac{1}{2}}}\right] + M(\tfrac{5}{6}, \tfrac{1}{2}, \hat{\phi})\int_{\hat{\phi}}^{\infty} U(\tfrac{5}{6}, \tfrac{1}{2}, t)\frac{\mathrm{d}t}{t^{\frac{3}{2}}}\right\}; \tag{5.40}$$

M denotes the Kummer's function, $U(\frac{5}{6}, \frac{1}{2}, \hat{\phi})$ ($\sim \hat{\phi}^{-\frac{5}{6}}$ as $\hat{\phi} \to \infty$) denotes a second functionally independent confluent hypergeometric function (Abramowitz & Stegun, 1964, p. 504), and Γ denotes the gamma function. It follows that

$$\hat{F}_{\mathrm{p}} \sim \frac{3}{4\hat{\eta}^2} \quad \text{as} \quad \hat{\eta} \to \pm\infty, \tag{5.41}$$

$$\hat{F}_{\mathrm{p}} \sim \ln|\hat{\eta}| + D_{\mathrm{p}} \quad \text{as} \quad \hat{\eta} \to 0, \tag{5.42}$$

where $D_{\mathrm{p}} = 0.51119877\ldots$. Equations (5.41) and (5.42) show that the particular solution (5.40) eliminates the logarithmic behaviour of the inner solution and converts it into an algebraic decay at infinity. This allows the critical-layer solution

to match onto the external solution. In fact, (5.1)–(5.4), (5.12), (5.13), (5.33)–(5.36), and (5.41) show that the outer diffusive solution matches the external flow to leading order, i.e. (4.22) of I is satisfied.

5.4. *Matching and the composite expansion*

Having constructed appropriate inner and outer solutions we must now show that they can be matched in some mutual overlap domain. This leads to conditions on the constants b_0, b_{0L}, $\hat{b}^{(0)}_{\gtrless}$, etc that appear in the expansions. In fact, (5.3), (5.12), (5.18)–(5.26), (5.33), (5.38), and (5.39) show that the inner and outer expansions (5.14) and (5.35), respectively, will match if

$$b_{0L} = \tfrac{1}{2}\alpha_\infty, \tag{5.43}$$

$$b_0 \mp \tfrac{1}{4} e_0 C^{(1)} - \alpha_\infty C^{(2)} = \alpha_\infty D_{\mathrm{p}} + \hat{b}^{(0)}_{\gtrless} \frac{\pi^{\frac{1}{2}}}{\Gamma(\frac{4}{3})} \tag{5.44}$$

where

$$\tfrac{1}{2}C^{(1)} = \int_2^\infty \left(\frac{2\pi}{I} - \frac{1}{\bar{\phi}^{\frac{1}{2}}}\right) \mathrm{d}\bar{\phi} - 8^{\frac{1}{3}} = -2.7575749\ldots, \tag{5.45}$$

(see Haberman 1972; Smith & Bodonyi 1982) and

$$2C^{(2)} = \int_2^\infty \left(\frac{2I_1}{I} + \frac{1}{\bar{\phi}}\right) \mathrm{d}\bar{\phi} - \ln 2 = 0.58931896\ldots. \tag{5.46}$$

The uniformly valid $O(1)$ composite expansion corresponding to (5.14) and (5.35) can, therefore, be written as

$$\bar{Q} = F^{(0)}(\hat{\phi}) + e_0 \bar{\eta} + \alpha_\infty [\hat{F}_{\mathrm{p}}(\hat{\phi}) - \ln|\bar{\eta}| - D_{\mathrm{p}}] + \hat{b}^{(0)}_{\gtrless} \left[\mathrm{e}^{-\hat{\phi}} U(\tfrac{5}{6}, \tfrac{1}{2}, \hat{\phi}) - \frac{\pi^{\frac{1}{2}}}{\Gamma(\frac{4}{3})}\right]. \tag{5.47}$$

5.5. *Mean-flow and velocity-change constraints*

Substituting (5.47) into the mean-flow constraint (5.7), noting that the dominant contribution to the integral comes from the outer region (i.e. $\hat{\eta} = O(1)$) and that, in this region, the overlap-domain terms cancel the inner-expansion terms in (5.47), we obtain, upon equating $O[(\bar{\lambda}\bar{x})^{-\frac{1}{6}}]$ terms,

$$2\alpha_\infty \int_0^\infty \hat{F}_{\mathrm{p}} \, \mathrm{d}\hat{\eta} + (\hat{b}^{(0)}_{>} + \hat{b}^{(0)}_{<}) \frac{\pi^{\frac{1}{2}}}{\Gamma(\frac{11}{6})} = 0. \tag{5.48}$$

Integrating the differential equation for $\hat{F}_{\mathrm{p}}$ by parts shows that the integral involving $\hat{F}_{\mathrm{p}}$ in (5.48) vanishes and, consequently, that

$$\hat{b}^{(0)}_{>} + \hat{b}^{(0)}_{<} = 0. \tag{5.49}$$

Hence, (5.44) and (5.49) show that

$$b_0 = \alpha_\infty (C^{(2)} + D_{\mathrm{p}}), \tag{5.50}$$

$$\hat{b}^{(0)}_{\gtrless} = \mp \frac{\Gamma(\frac{4}{3})\, e_0 C^{(1)}}{4\pi^{\frac{1}{2}}}. \tag{5.51}$$

Substitution of (5.47) into the real part of (5.6), i.e. the velocity-jump constraint, equating $O(1)$ terms, changing the order of integration using (5.8), integrating by parts, and again changing the order of integration leads to

$$\theta'_\infty = 2\alpha_\infty C^{(3)}, \tag{5.52}$$

where

$$C^{(3)} = \frac{1}{\pi}\int_2^{+\infty} \frac{I_1^2}{I}\,\mathrm{d}\bar{\phi} = 2.721391\,86\ldots. \tag{5.53}$$

5.6. *The cat's-eye boundary layer and the phase-jump condition*

While we have required that $Q^{(0)}$ be continuous across the cat's-eye boundary $\bar{\phi} = 2$, its higher derivatives will, in general, be discontinuous, and this induces a higher-order viscous boundary layer of the type considered by Brown & Stewartson (1978) (see figure 1). In fact, it follows from (5.29), (5.30), and (5.32) that

$$F^{(0)} = b_0 + \Gamma(\bar{\phi}-2) + O[(\bar{\phi}-2)^2 \ln|\bar{\phi}-2|] \quad \text{as} \quad \bar{\phi}\to 2, \tag{5.54}$$

where

$$\Gamma = \Gamma_{\gtrless} = \mp\tfrac{1}{8}\pi\, \mathrm{e}_0 + \tfrac{1}{3}\alpha_\infty \quad \text{for} \quad \bar{\phi}\to 2+, \quad \bar{\eta} \gtrless 0, \tag{5.55}$$

$$\Gamma = \Gamma_- = \tfrac{1}{3}\alpha_\infty \quad \text{for} \quad \bar{\phi}\to 2-. \tag{5.56}$$

To smooth these discontinuities in the first derivative of $F^{(0)}$, we introduce the scaled variables

$$T = -\operatorname{sgn}\bar{\eta}\,\cos\tfrac{1}{2}\bar{X}, \tag{5.57}$$

$$N = \tfrac{1}{4}(a_\infty^{\frac{3}{2}}\bar{x})^{\frac{1}{2}}(\bar{\phi}-2), \tag{5.58}$$

$$\bar{Q} = \mathrm{e}_0\,\bar{\eta} + b_0 + \frac{4\tilde{Q}}{(a_\infty^{\frac{3}{2}}\bar{x})^{\frac{1}{2}}}, \tag{5.59}$$

describing the internal shear layer(s) centred about $\bar{\phi} = 2$. To lowest approximation, (5.5) then becomes the diffusion equation

$$\frac{\partial\tilde{Q}}{\partial T} = \frac{\partial^2\tilde{Q}}{\partial N^2}, \quad -1 < T < 1, \tag{5.60}$$

subject to

$$\tilde{Q}\to\Gamma N \quad \text{as} \quad |N|\to+\infty, \tag{5.61}$$

in order for its solution to match with (5.54).

The initial conditions at the saddle point $T = -1$ are obtained from compatibility requirements between the individual solutions for the four cat's-eye boundary layers that come together there (Benney & Bergeron 1969). This leads to a Wiener–Hopf problem that can be reduced to a problem shown by Brown & Stewartson (1978) to have a solution. (In contrast, the Wiener–Hopf problem considered by Benney & Bergeron (1969) does not possess a solution, Brown & Stewartson (1978)). We do not pursue these issues further but go on to show how e_0 is related to a_∞ by considering the phase-jump condition, i.e. the imaginary part of (5.6).

To this end we first note that

$$\bar{Q} = \bar{Q}_1 + \frac{4}{(a_\infty^{\frac{3}{2}}\bar{x})^{\frac{1}{2}}}[\tilde{Q}(T,N) - \Gamma N] + \ldots, \tag{5.62}$$

where $\bar{Q}_I$ is given by (5.14), is a uniformly valid composite expansion for $\bar{Q}$ everywhere except as $|\bar{\eta}| \to +\infty$. This non-uniformity can be removed, as above, by considering the outer diffusive region. However, it does not effect the present development and is, therefore, ignored.

Substituting (5.14), (5.57), (5.58), and (5.62) into (5.6) and equating the imaginary part to zero we find that the resulting equation is identically satisfied up to (but not including) $O[(\bar{\lambda}\bar{x})^{-1}]$. Equating the coefficient of $(\bar{\lambda}\bar{x})^{-1}$ to zero leads to an equation consisting of the sum of two integrals equalling a constant; one of the integrals involves $Q^{(6)}$ and the other involves $\tilde{Q}$. Inserting (5.21) in the first integral, then changing the variable of integration from $\bar{\eta}$ to $\bar{\phi}$, using (5.8), integrating by parts first with respect to $\bar{X}$ and then with respect to $\bar{\phi}$, and, for the other integral, changing the variables as indicated in (5.57) and (5.58) leads to

$$e_0(C^{(1)}+2\pi)+\frac{16}{\pi}\int_{-\infty}^{+\infty}\int_{-1}^{1}\frac{T}{(1-T^2)^{\frac{1}{2}}}[\tilde{Q}_>-\tilde{Q}_<-H(N)(\Gamma_>-\Gamma_<)N]\,\mathrm{d}T\,\mathrm{d}N=\frac{2a_\infty^{\frac{3}{2}}}{3}, \tag{5.63}$$

where $H(N)$ is the unit step function. The first term on the left-hand side arises from the integral involving $Q^{(6)}$. The second term arises from the $\tilde{Q}$-integral and involves the solution to the boundary-value problem (5.59) and (5.60) which, in turn, depends on the parameters $\Gamma_{\gtrless}$ and Γ_-. This problem was solved by Brown & Stewartson (1978) in the special case where $\Gamma_- = 0$. Inspection of their solution shows that terms involving Γ_- cancel out in the integral in (5.63), which therefore depends only on $\Gamma_> - \Gamma_<$. In fact, it turns out that this integral exactly cancels the $2\pi e_0$ term in (5.63) (see also Smith & Bodonyi 1982) so that this equation becomes

$$3e_0 C^{(1)} = 2a_\infty^{\frac{3}{2}}. \tag{5.64}$$

5.7. *The amplitude and phase coefficients*

We have now shown that the inner and outer asymptotic expansions (5.14) and (5.35) satisfy the integral constraints (5.6), (5.7), and (5.11) to the appropriate order as long as the amplitude and phase coefficients a_∞ and θ'_∞, respectively, satisfy (5.52) and (5.64). Combining (5.16), (5.22) with these two equations yields

$$a_\infty = \left[\frac{3|C^{(1)}|}{2(1+\bar{U}^2 D)}\right]^{\frac{2}{3}}, \tag{5.65}$$

$$\theta'_\infty = \frac{2\bar{U}D}{1+\bar{U}^2 D}, \tag{5.66}$$

where

$$D = -C^{(1)}C^{(3)}/4 = 3.7522095\ldots. \tag{5.67}$$

The other constants in the leading-order solution, i.e. b_{0L}, b_0, and $\hat{b}_{\gtrless}^{(0)}$, can now be evaluated for a given value of $\bar{U}$ by using (5.16), (5.22), (5.43), (5.50), (5.51), (5.65), and (5.66).

The analysis can be continued to obtain the next-order terms in (5.12) and (5.13). We omit the details and give only the final results for a_1 and θ_1, i.e.

$$a_1 = \frac{2a_\infty^2}{15}\left[\frac{\Gamma(\frac{4}{3})}{\Gamma(\frac{5}{6})} - \bar{U}^2 C^{(4)}\right], \tag{5.68}$$

$$\theta_1 = \frac{a_\infty^2}{6}\left[\frac{\Gamma(\frac{4}{3})}{\Gamma(\frac{5}{6})} + \frac{C^{(4)}}{D}\right], \tag{5.69}$$

where

$$C^{(4)} = \int_0^{+\infty}\left(\hat{F}_{\mathrm{p}}' - \frac{1}{\hat{\eta}}\right)\frac{\mathrm{d}\hat{\eta}}{\hat{\eta}} = -1.9519525\ldots. \tag{5.70}$$

6. Numerical results

The principal result of the previous section is the formulas (5.45) and (5.65)–(5.70) giving the numerical values of the coefficients in the asymptotic expansions (5.12) and (5.13) of the complex amplitude $A = ae^{-i\Theta}$ of the leading-order outer instability-wave solution, cf. (2.27). Equations (5.12) and (5.65) show that, consistently with the Huerre & Scott (1980) equilibrium critical-layer analysis, $|A|$ grows like $(\bar{\lambda}\bar{x})^{\frac{2}{3}}$, but that the numerical coefficient in our result differs from theirs by a factor of $(1+\bar{U}^2 D)^{-\frac{2}{3}}$.

Figure 2 shows the numerically computed local (scaled) growth rate, $\mathrm{d}(\ln|A|)/\mathrm{d}\bar{x}$, as a function of the scaled (and shifted) streamwise coordinate $\bar{x}$ for various values the viscous parameter $\bar{\lambda}$. Also shown are the linear viscous growth rate and the inviscid ($\bar{\lambda} = 0$) nonlinear growth rate. Part (a) corresponds to the case $\bar{U} = 1$, where the lower stream has zero velocity and part (b) to the case $\bar{U} = 3$. It can be seen that $\mathrm{d}(\ln|A|)/\mathrm{d}\bar{x}$ initially equals the linear growth rate κ_{r} but is then very rapidly reduced by the nonlinear effects. But rather than continuing to oscillate about zero, as the inviscid solution appears to do, the oscillation of the local growth rate is diminished with increasing $\bar{x}$ and there is a reduction in the bias towards growth, consistently with (5.12). This is shown more clearly in figure 3, where $\ln|A|$ is shown as a function of $\ln(\bar{\lambda}\bar{x})$ (with (a) corresponding to $\bar{U} = 1$ and (b) to $\bar{U} = 3$). The dashed curves in this figure are calculated from the first two terms in the asymptotic solution (5.12). The second term was needed to obtain good agreement with the numerical computations, which would have been prohibitively expensive to extend much further downstream. This figure suggests that the approach to the ultimate quasi-equilibrium state is quite slow [the next-order term in (5.12) varies like $(\bar{\lambda}\bar{x})^{\frac{1}{3}}$] and that the quasi-equilibrium asymptotic state acts as a kind of attractor for the non-equilibrium (growth-dominated) solutions when $\bar{\lambda}\bar{x}$ becomes large.

At a fixed $\bar{x}$, the instability-wave amplitude increases with increasing $\bar{\lambda}$, which basically means increasing viscosity. This might, at first, seem rather surprising, but as indicated in the introduction, the instability-wave growth rate is always proportional to the phase jump across the critical layer. Nonlinear effects drive the phase jump, and consequently the growth rate, toward zero (Gajjar & Smith 1985; Goldstein & Durbin 1986; Goldstein *et al.* 1987; Goldstein & Leib 1988) Viscosity, on the other hand, tends to keep the critical-layer phase jump from vanishing and thereby causes the final instability wave to increase.

Figure 4 shows the numerically computed phase variation Θ' versus the scaled streamwise coordinate $\bar{\lambda}\bar{x}$, with (a) corresponding to $\bar{U} = 1$ and (b) to $\bar{U} = 3$. The dashed curves are computed from the first two terms in the asymptotic expansion

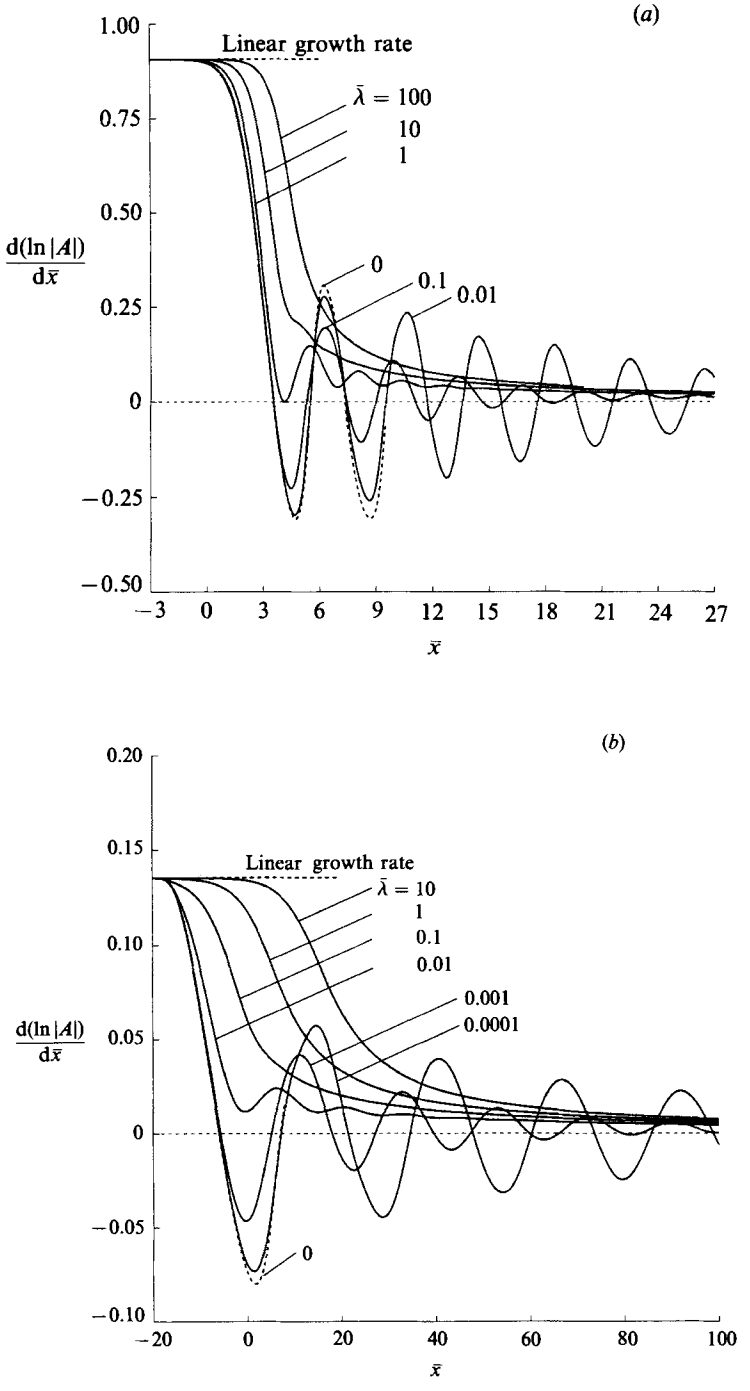

FIGURE 2. Scaled growth rate of fundamental instability wave as a function of slow streamwise distance for various values of the viscous parameter λ. Dashed curves: $\lambda = 0$ (inviscid) and linear growth rates. (*a*) $\bar{U} = 1$; (*b*) $\bar{U} = 3$.

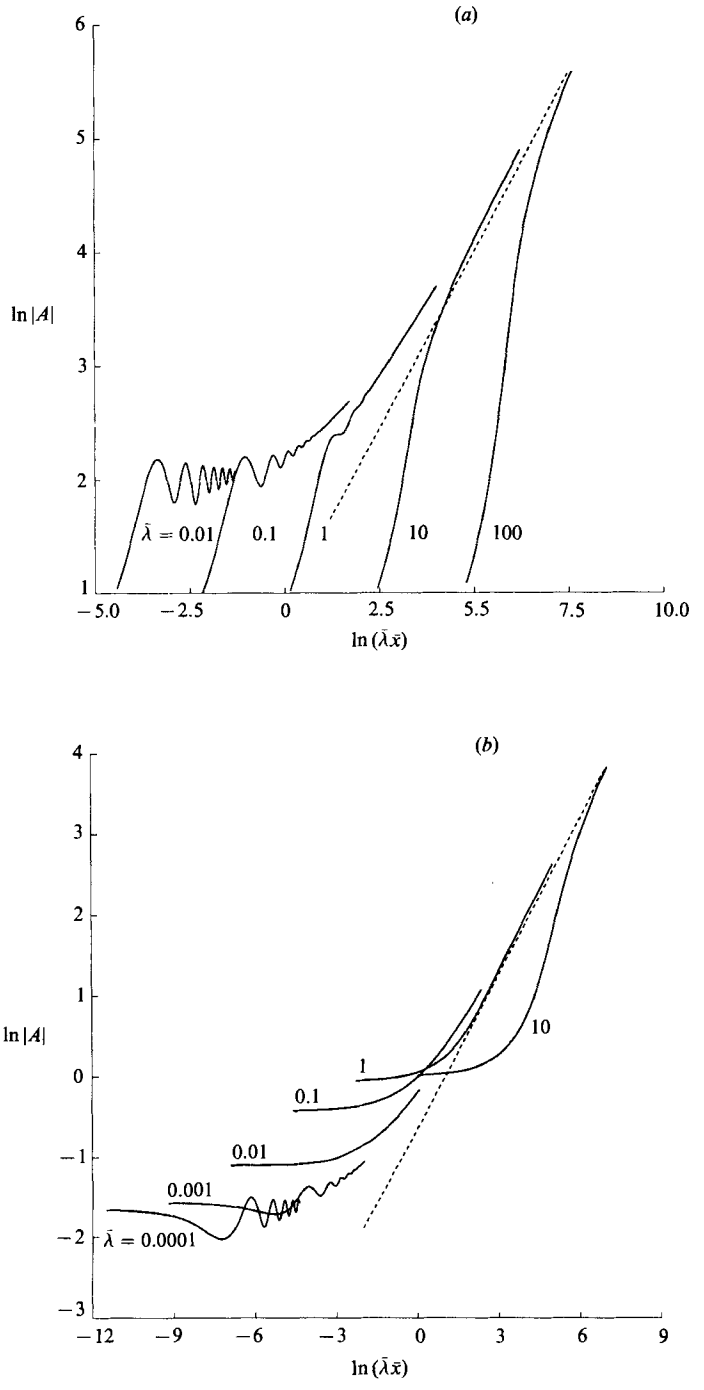

FIGURE 3. Scaled fundamental instability-wave amplitude as a function of slow streamwise distance times the viscous parameter $\bar{\lambda}$ for various values of λ. Solid curves: numerical solution of non-equilibrium vorticity equation. Dashed curves: two-term asymptotic expansion (5.12). (*a*) $\bar{U} = 1$; (*b*) $\bar{U} = 3$.

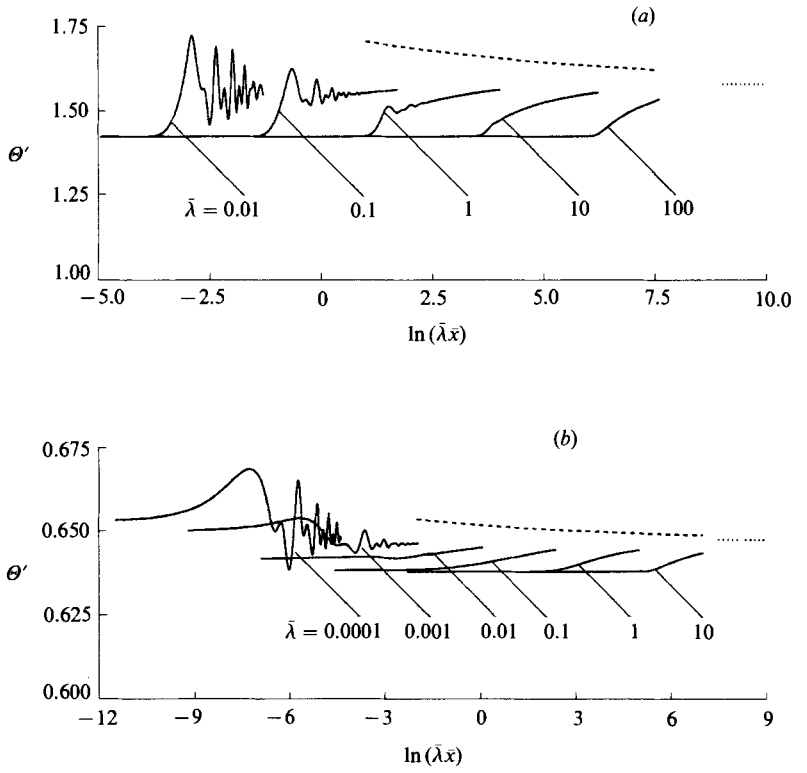

FIGURE 4. Scaled wavenumber of the instability-wave amplitude $\Theta' = \mathrm{Im}(-A'/A)$ as a function of slow streamwise distance times the viscous parameter $\bar{\lambda}$ for various values of $\bar{\lambda}$. Solid curves: numerical solution of non equilibrium vorticity equation. Dashed curves: two-term asymptotic expansion (5.13). Dotted curves: leading-order asymptotic result θ'_{∞}.

(5.13) and the dotted curves correspond to the first term only. It can be seen that the numerical results slowly approach this universal result for all $\bar{\lambda} > 1$. It is worth noting that the Huerre & Scott (1980) result implies that $\Theta' \equiv 0$ as $\bar{\lambda}\bar{x} \to \infty$ and is therefore not consistent with our numerical computations.

Figure 5 is a plot of constant-vorticity lines in the (X, η)-plane at various values of $\bar{x}$ for $\bar{U} = 1$ and $\bar{\lambda} = 0.01$. The overall behaviour, in this case, is similar to the inviscid case described in I. The contours actually correspond to constant values of

$$-4\Omega_1/\bar{U}^2 S_1^2 - 2\bar{\lambda}(\bar{x}+x_0) = (\eta - 2/\bar{U})^2 + 2\mathrm{Re}\,(A\,\mathrm{e}^{\mathrm{i}X}) - 4Q/\bar{U}. \tag{6.1}$$

The first term on the left-hand side is the actual rescaled $O(\epsilon)$-critical-layer vorticity perturbation [cf. (3.7), (3.9)–(3.15)]; the second term is a (now suppressed) change in the overall contour level between the different parts of each figure. Figure 6 is the same as figure 5 but with the scaled viscous parameter $\bar{\lambda}$ equal to unity. The initial vorticity roll-up is still basically inviscid, but it ultimately departs from this behaviour and develops the simpler patterns shown in the last parts of the figure. These latter patterns are consistent with the asymptotic solution constructed in §5.

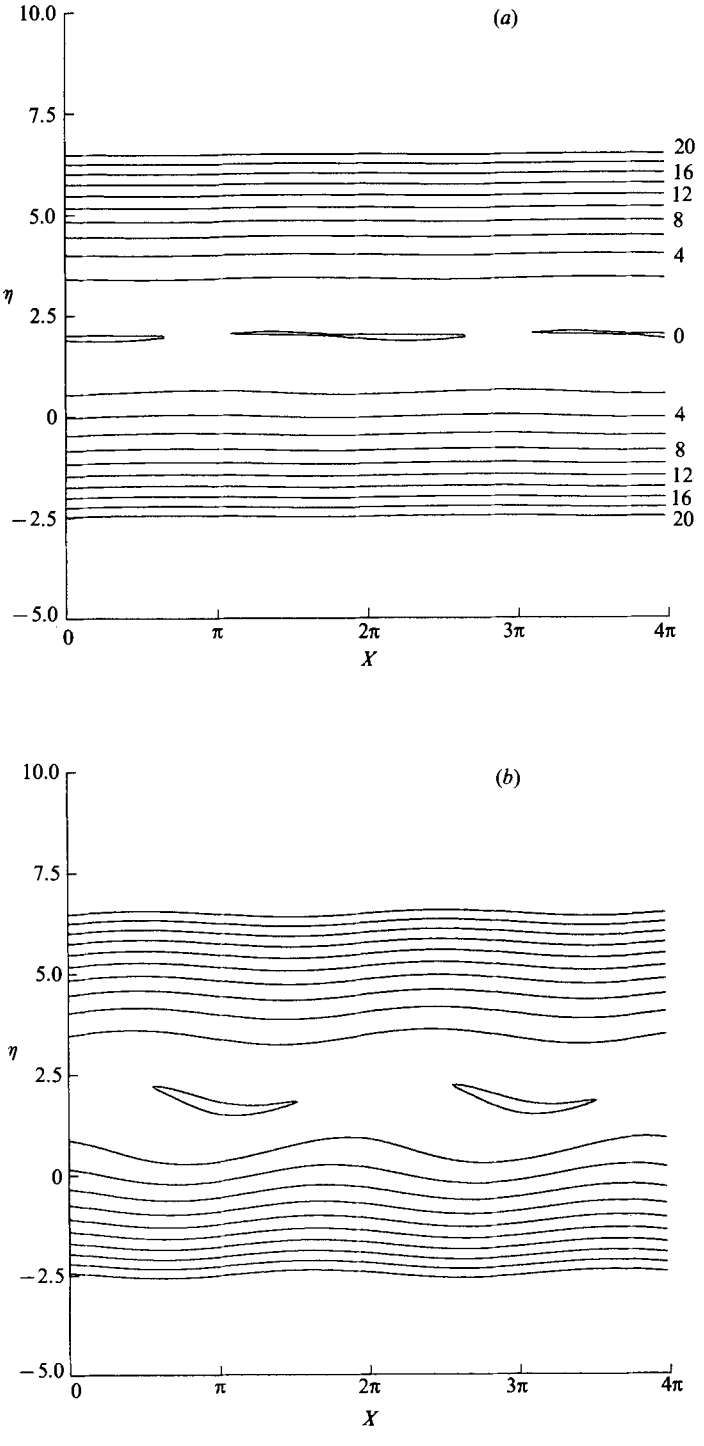

FIGURE 5(*a*, *b*). For caption see next page.

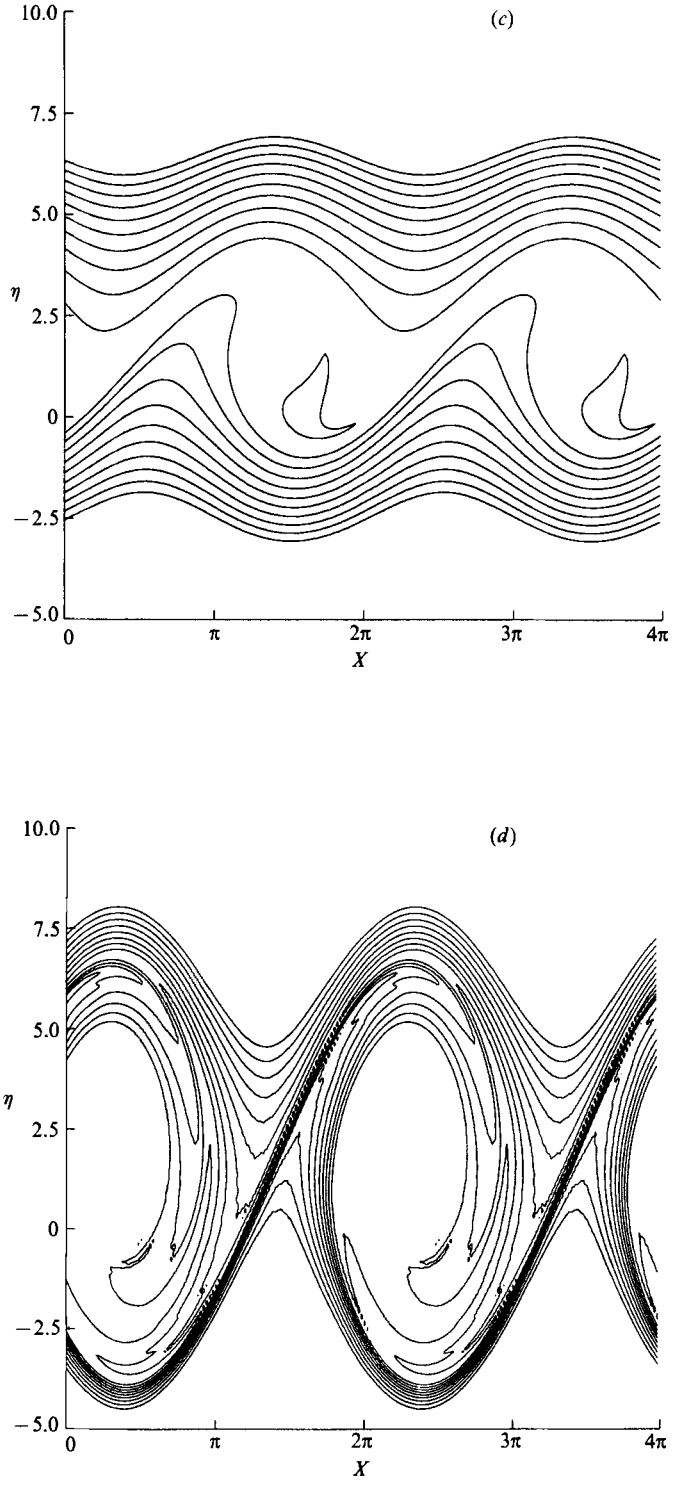

FIGURE 5. Vorticity contours in the (X, η)-plane for $\bar{U} = 1$ and $\bar{\lambda} = 0.01$ $[\eta = -2(Y - S_1)/S_1\bar{U}$, $X = x - (\bar{U} + \epsilon^{\frac{1}{2}}S_1)t - X_0]$. (*a*) $\bar{x} = -3$; (*b*) $\bar{x} = -1$; (*c*) $\bar{x} = 1$; (*d*) $\bar{x} = 3$. Contour levels (cf. (6.1)) are given in (*a*).

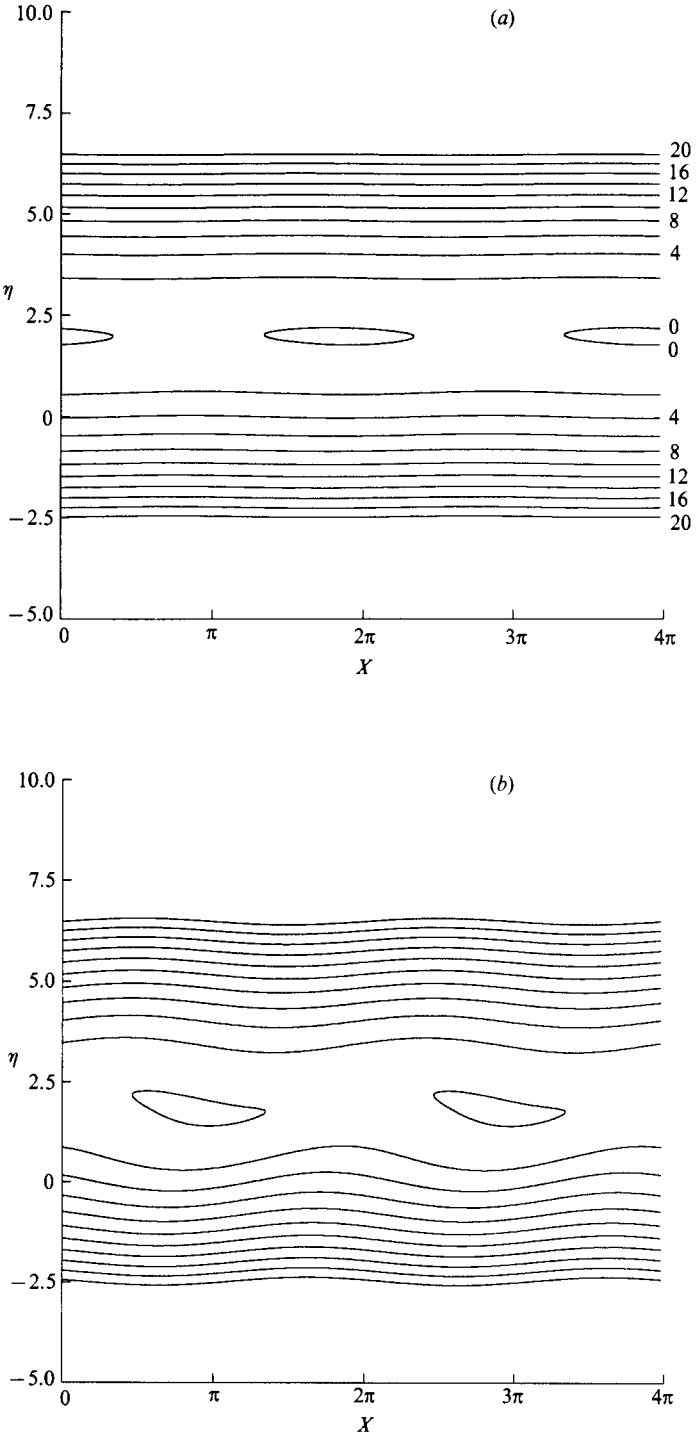

FIGURE 6(*a*, *b*). For caption see p. 322.

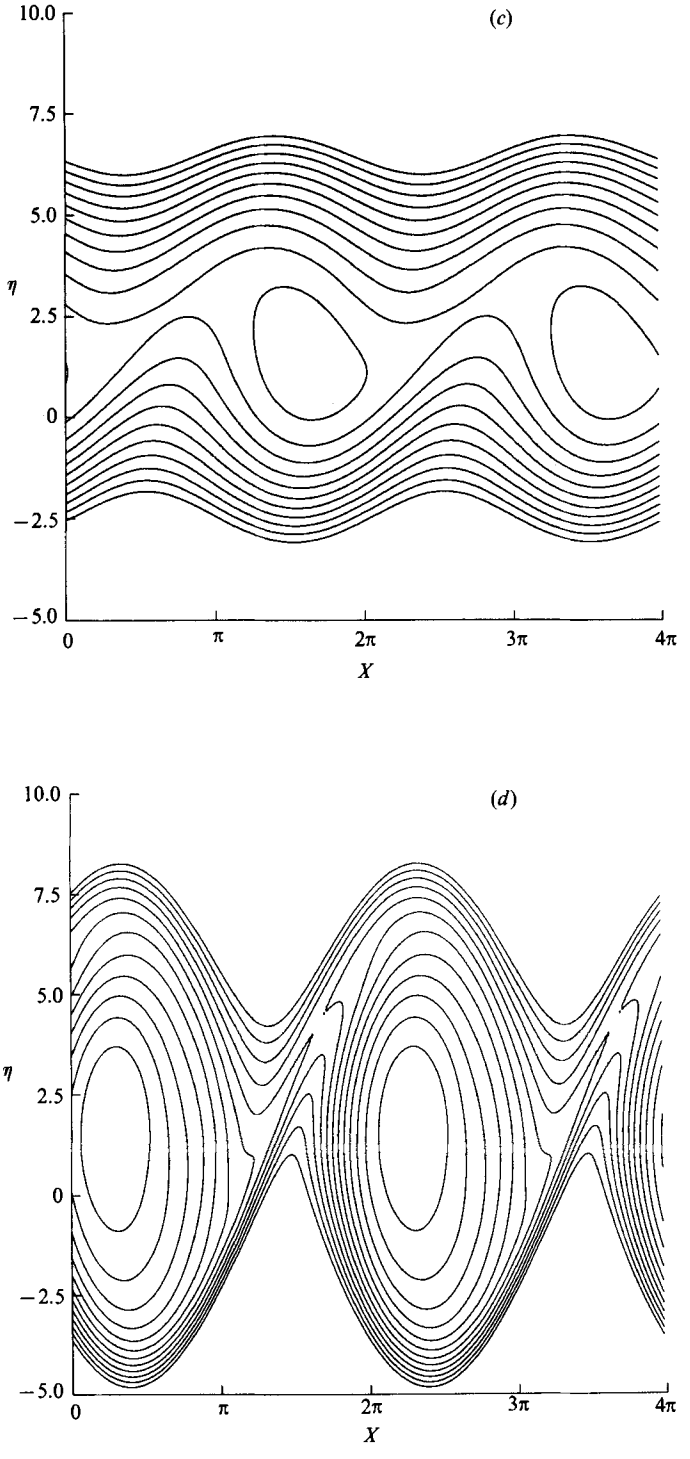

FIGURE 6(*c*,*d*). For caption see p. 322.

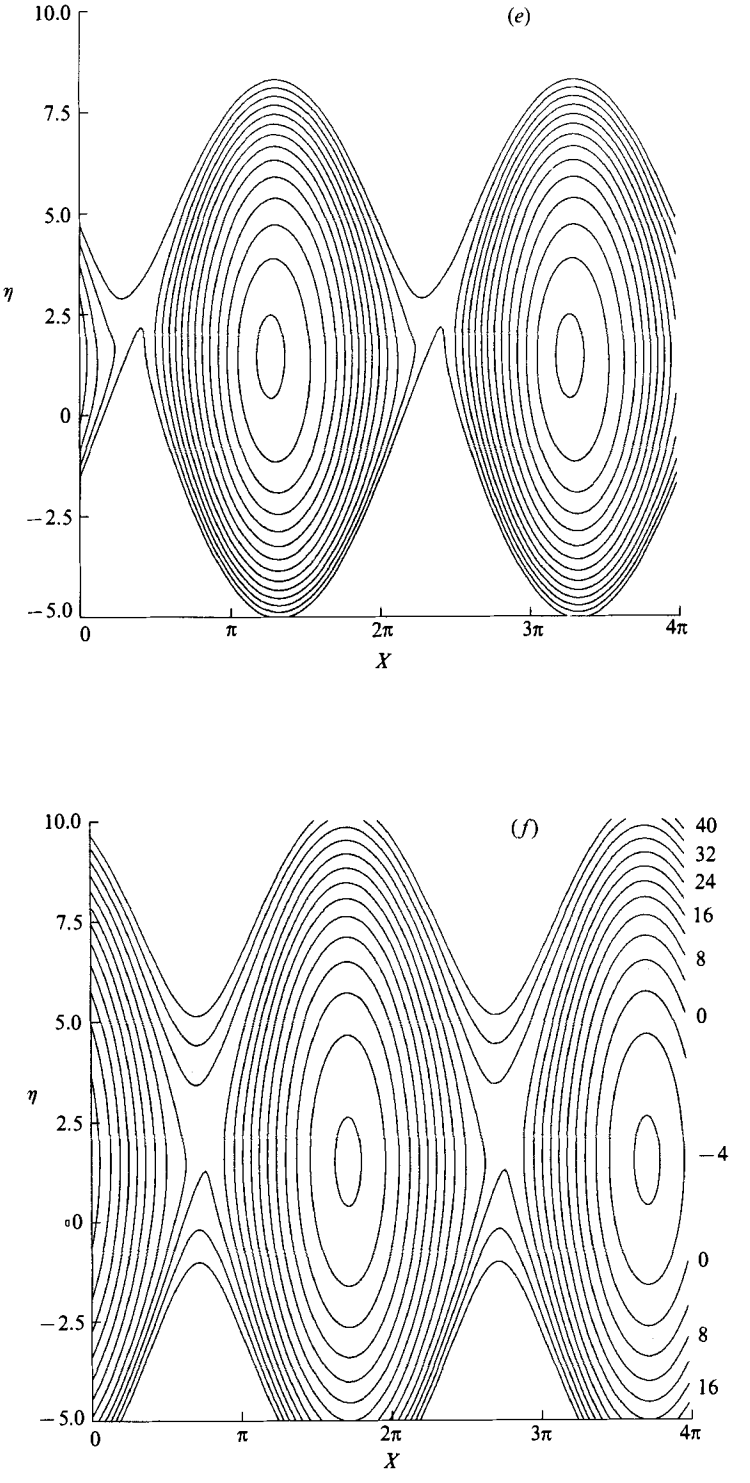

FIGURE 6. Same as figure 5, except $\bar{\lambda} = 1$. (*a*) $\bar{x} = -3$; (*b*) $\bar{x} = -1$; (*c*) $\bar{x} = 1$; (*d*) $\bar{x} = 3$; (*e*) $\bar{x} = 5$; (*f*) $\bar{x} = 10$. Contour levels (cf. (6.1)) for (*a–e*) are given in (*a*).

7. The next stage of evolution

The progressively increasing local approximation (2.32) to the viscous mean-flow change will eventually alter the critical-layer structure and thereby induce an $O(x_1 \epsilon^{\frac{1}{2}}/A^{\dagger\frac{3}{2}})$ correction to the local instability-wave growth rate, $\mathrm{d} \ln A^{\dagger}/\mathrm{d}x_1$. Since the relatively slow algebraic growth of that wave allows this to occur before the instability-wave amplitude becomes $O(1)$, the critical-layer expansion (3.3) will first break down when this correction becomes of the same order of magnitude as the local asymptotic instability-wave growth rate, i.e. $O(1/x_1)$, see (5.12). This occurs when $x_1 = O(\epsilon^{-\frac{1}{2}})$, or, equivalently, when $x_3 = O(\epsilon)$ (see figure 1).

The equations have to be rescaled in this next stage of evolution, but the flow should still behave linearly in the main part of the shear layer with the nonlinear effects again confined to a narrow critical layer, since the instability-wave amplitude is still only $O(\epsilon^{\frac{2}{3}})$. The critical layer now has thickness $O(\epsilon^{\frac{1}{3}})$ and, as shown below, moves across the shear layer in order to remain in the quasi-equilibrium state achieved asymptotically in the previous stage.

The analysis of this next stage of evolution is in many respects similar to that of §§2 and 5. The expansion in the main part of the shear layer is, to a large extent, a simple reordering of the expansion of §2. The analysis in §5 can be modified to solve the relevant critical-layer problems and thus to determine the amplitude and phase variations in this stage.

7.1. *Expansion in the main part of the shear layer*

The previous discussion suggests that the solution in the main shear layer should now expand like

$$\psi = \psi_0 + \epsilon^{\frac{1}{2}} 2\lambda x_2 G(y) + \epsilon^{\frac{2}{3}} A_\infty(x_2)\,\mathrm{sech}\, y \cos\left(\zeta - \frac{\Theta_\infty(x_2)}{\epsilon^{\frac{1}{2}}}\right) + \epsilon(\lambda x_2)^2 G^{(1)}(y) + \epsilon^{\frac{7}{6}}\psi_{\frac{7}{6}} + \epsilon^{\frac{4}{3}}\psi_{\frac{4}{3}} + \epsilon^{\frac{3}{2}}(\lambda x_2)^3 G^{(2)}(y) + \epsilon^{\frac{5}{3}}\psi_{\frac{5}{3}} + \ldots, \quad (7.1)$$

where ψ_0 is the basic flow of §2; G and ζ are given by (2.33) and (2.16) respectively; $G^{(1)}$ and $G^{(2)}$ are the y-dependent coefficients in the Taylor-series expansion of the basic-flow stream function; A_∞ and Θ_∞ are real functions of x_2; and

$$x_2 = \epsilon^{\frac{1}{2}} x_1 = \epsilon x \quad (7.2)$$

is a new scaled streamwise coordinate, which is $O(1)$ in the region of interest.

In order to ensure that the downstream expansion (7.1) matches onto the non-equilibrium expansion (2.17) we must require that (cf. (2.27), (3.10), (3.13), (3.15), (5.1), (5.12), and (5.13))

$$A_\infty \to a_\infty \left(\frac{\lambda |S_1| x_2}{2}\right)^{\frac{2}{3}}, \quad (7.3)$$

$$\Theta_\infty \to \frac{|S_1| \theta'_\infty x_2}{2}, \quad (7.4)$$

as $x_2 \to 0$, where a_∞ and θ'_∞ are given by (5.65) and (5.66).

The $O(\epsilon^{\frac{7}{6}})$-term is now determined by

$$\mathscr{L}_0 \psi_{\frac{7}{6}} = -\left[2\lambda x_2 \left(G''' - \frac{U''}{U} G'\right) + \Theta'_\infty \left(\bar{U}\frac{U''}{U} - 2U\right) + S_1 \frac{U''}{U}\right] A_\infty \,\mathrm{sech}\, y \sin\left(\zeta - \frac{\Theta_\infty(x_2)}{\epsilon^{\frac{1}{2}}}\right), \quad (7.5)$$

where $\mathscr{L}_0$ is given by (2.23). The solution of (7.5) is

$$\psi_{\frac{7}{6}} = \Phi_{\frac{7}{6}}(y, x_2)\cos\left(\zeta - \frac{\Theta_\infty(x_2)}{\epsilon^{\frac{1}{2}}}\right), \tag{7.6}$$

where

$$\begin{aligned}\Phi_{\frac{7}{6}} = {} & a_{\frac{7}{6}}\operatorname{sech} y + b_{\frac{7}{6}}^{\pm}(y\operatorname{sech} y + \sinh y)\\ & + A_\infty\{(\bar{U}\Theta'_\infty + S_1)[\operatorname{sech} y\,\chi_2(\tanh y) - (y\operatorname{sech} y + \sinh y)\ln|\tanh y|]\\ & - \Theta'_\infty\tanh y\sinh y\} - \lambda x_2 A_\infty\{2c_1^{(0)}\tanh y\operatorname{sech} y + (\chi_1 - \chi_4)\operatorname{sech} y\\ & + (y\operatorname{sech} y + \sinh y)[\chi_3 - \tfrac{1}{2}\operatorname{sech}^2 y - \tfrac{1}{2}\operatorname{cosech} y\operatorname{sech} y\,\chi_1 - \frac{1}{\bar{U}^2}\ln|\tanh y|]\},\end{aligned} \tag{7.7}$$

$$\chi_1 = 2\operatorname{sech} y\operatorname{cosech} y\ln\left(\frac{\bar{U} + \tanh y}{\bar{U}}\right), \tag{7.8}$$

$$\chi_2(s) = \int_0^s \frac{\tanh^{-1} t}{t}\,\mathrm{d}t, \tag{7.9}$$

$$\chi_3 = \left(\bar{U} - \frac{1}{\bar{U}}\right)^2\ln\left(\frac{\bar{U} + \tanh y}{\bar{U}}\right) - \bar{U}\tanh y - \frac{1}{\bar{U}\tanh y}, \tag{7.10}$$

$$\chi_4 = \int_0^y [y(\operatorname{sech}^2 y + \operatorname{cosech}^2 y) - \operatorname{cosech} y\operatorname{sech} y]\chi_1(y)\,\mathrm{d}y. \tag{7.11}$$

The solution $\Phi_{\frac{7}{6}}$ can only vanish at infinity if

$$b_{\frac{7}{6}}^{\pm} \mp A_\infty\Theta'_\infty = \lambda x_2 A_\infty\chi_3(\pm\infty), \tag{7.12}$$

which leads to the $O(\epsilon^{\frac{7}{6}})$-jump condition

$$b_{\frac{7}{6}}^{+} - b_{\frac{7}{6}}^{-} = 2A_\infty\Theta'_\infty + \lambda x_2 A_\infty[\chi_3(+\infty) - \chi_3(-\infty)]. \tag{7.13}$$

This determines the leading-order velocity-jump condition across the critical layer.

The $O(\epsilon^{\frac{4}{3}})$-term in (7.1), is determined by

$$\mathscr{L}_0\psi_{\frac{5}{6}} = -A'_\infty\operatorname{sech}^5 y\sinh y\cos\left[2\left(\zeta - \frac{\Theta_\infty(x_2)}{\epsilon^{\frac{1}{2}}}\right)\right]. \tag{7.14}$$

The solution to (7.14) consists of a mean-flow correction term and a second-harmonic term, neither of which play any dynamically significant role in the analysis.

The $O(\epsilon^{\frac{5}{3}})$-term in (7.1) satisfies

$$\mathscr{L}_0\psi_{\frac{5}{6}} = -A'_\infty\left(\bar{U}\frac{U''}{U} - 2U\right)\operatorname{sech} y\cos\left(\zeta - \frac{\Theta_\infty(x_2)}{\epsilon^{\frac{1}{2}}}\right) + \mathrm{OT}, \tag{7.15}$$

where OT denotes out-of-phase terms, i.e. terms proportional to $\sin(\zeta - \Theta_\infty(x_2)/\epsilon^{\frac{1}{2}})$. These latter terms do not play a role in the determination of the amplitude and phase to the order of approximation of the analysis and, for simplicity of presentation, are therefore ignored in what follows. The solution to (7.15) is then

$$\psi_{\frac{5}{3}} = \Phi_{\frac{5}{3}}\sin\left(\zeta - \frac{\Theta_\infty(x_2)}{\epsilon^{\frac{1}{2}}}\right), \tag{7.16}$$

where

$$\Phi_{\frac{5}{3}} = a_{\frac{5}{3}} \operatorname{sech} y + b_{\frac{5}{3}}^{\pm}(y \operatorname{sech} y + \sinh y)$$
$$+ A'_{\infty}\{\bar{U}[(y \operatorname{sech} y + \sinh y) \ln|\tanh y| - \operatorname{sech} y\, \chi_2(\tanh y)] + \tanh y \sinh y\}. \quad (7.17)$$

$\Phi_{\frac{5}{3}}$ can only vanish at infinity if

$$b_{\frac{5}{3}}^{\pm} \pm A'_{\infty} = 0, \quad (7.18)$$

leading to the $O(\epsilon^{\frac{5}{3}})$ jump condition

$$b_{\frac{5}{3}}^{+} - b_{\frac{5}{3}}^{-} = -2A'_{\infty}, \quad (7.19)$$

which determines the phase jump across the critical layer to leading order.

Without going into detail, it is sufficient to note that the outer expansion is again singular at the origin and that a new critical-layer expansion has to be introduced to determine the jumps (7.13) and (7.19).

7.2. *Critical-layer expansion*

Inspection of the singularity occurring in the expansion (7.1) as $y \to 0$ shows that the critical-layer thickness is now $O(\epsilon^{\frac{1}{3}})$. We therefore introduce the stretched transverse variable

$$\bar{Y} = y/\epsilon^{\frac{1}{3}} \quad (7.20)$$

and note that the inner expansion of the outer solution (7.1) suggests that the critical-layer solution will expand like

$$\Psi = \epsilon^{\frac{1}{2}} 2\lambda x_2 \bar{U} c_1^{(0)} + \epsilon^{\frac{2}{3}}(\Psi_0 + \epsilon^{\frac{1}{6}}\Psi_{\frac{1}{6}} + \epsilon^{\frac{1}{3}}\Psi_{\frac{1}{3}} + \epsilon^{\frac{1}{2}}\Psi_{\frac{1}{2}} + \epsilon^{\frac{2}{3}}\Psi_{\frac{2}{3}}$$
$$+ \epsilon^{\frac{5}{6}} \ln\epsilon\, \Psi_{\frac{5}{6}L} + \epsilon^{\frac{5}{6}}\Psi_{\frac{5}{6}} + \epsilon\Psi_1 + \epsilon^{\frac{7}{6}}\Psi_{\frac{7}{6}} + \epsilon^{\frac{4}{3}}\Psi_{\frac{4}{3}} \ldots), \quad (7.21)$$

where the $O(\epsilon^{\frac{1}{3}})$-term and Ψ_0 to $\Psi_{\frac{5}{6}L}$ are simply re-expansions of the outer (main-region) solution. The remaining terms are non-trivial, but only $\Psi_{\frac{5}{6}}$ and the out-of-phase part of $\Psi_{\frac{4}{3}}$ play a dynamically significant role in determining the instability amplitude and phase to lowest order. These two quantities are determined by

$$\mathscr{L}_e \Omega_{\frac{5}{6}} = 2(\bar{U}\Theta'_{\infty} + S_1 - 2\lambda x_2 c_1^{(0)}) A_{\infty} \sin\left(\zeta - \frac{\Theta_{\infty}(x_2)}{\epsilon^{\frac{1}{2}}}\right), \quad (7.22)$$

$$\mathscr{L}_e \Omega_{\frac{4}{3}} = \lambda \frac{\partial^2 \Omega_{\frac{5}{6}}}{\partial \bar{Y}^2} + 2\bar{U}A'_{\infty} \cos\left(\zeta - \frac{\Theta_{\infty}(x_2)}{\epsilon^{\frac{1}{2}}}\right), \quad (7.23)$$

where $\mathscr{L}_e$ denotes the equilibrium critical-layer vorticity operator

$$\mathscr{L}_e = \bar{Y}\frac{\partial}{\partial\zeta} + A_{\infty} \sin\left(\zeta - \frac{\Theta_{\infty}(x_2)}{\epsilon^{\frac{1}{2}}}\right)\frac{\partial}{\partial \bar{Y}}, \quad (7.24)$$

$\Omega_{\frac{5}{6}} = \partial^2 \Psi_{\frac{5}{6}}/\partial\bar{Y}^2$ and $\Omega_{\frac{4}{3}}$ are minus the $O(\epsilon^{\frac{5}{6}})$- and minus the out-of-phase component of the $O(\epsilon^{\frac{4}{3}})$-critical-layer vorticity, respectively – note that we are only considering the out-of-phase component in (7.23).

Matching with the outer expansion (7.1) requires that the solutions to these equations satisfy the transverse boundary conditions

$$\Omega_{\frac{5}{6}} \to 2\lambda x_2(1/\bar{U}^2 - 2c_1^{(0)})\,\bar{Y}, \quad (7.25)$$

$$\Omega_{\frac{4}{3}} \to 0, \quad (7.26)$$

as $|\bar{Y}| \to \infty$, together with the integral constraints

$$\frac{1}{2\pi}\int_0^{2\pi}\int_{-\infty}^{+\infty} \Omega_{\frac{5}{6}} \cos\left(\zeta - \frac{\Theta_\infty(x_2)}{\epsilon^{\frac{1}{2}}}\right) \mathrm{d}\zeta\, \mathrm{d}\bar{Y} = b_{\frac{7}{6}}^{+} - b_{\frac{7}{6}}^{-}$$
$$= 2A_\infty [2\Theta'_\infty + \lambda x_2(\chi_3(+\infty) - \chi_3(-\infty))], \quad (7.27)$$

$$\frac{1}{2\pi}\int_0^{2\pi}\int_{-\infty}^{+\infty} \Omega_{\frac{4}{3}} \sin\left(\zeta - \frac{\Theta_\infty(x_2)}{\epsilon^{\frac{1}{2}}}\right) \mathrm{d}\zeta\, \mathrm{d}\bar{Y} = b_{\frac{5}{3}}^{+} - b_{\frac{5}{3}}^{-} = -2A'_\infty. \quad (7.28)$$

This boundary-value problem can effectively be converted into the one of §5 by introducing the new variables

$$\bar{X}_\infty = \zeta - \Theta_\infty(x_2)/\epsilon^{\frac{1}{2}}, \quad (7.29)$$

$$\bar{\eta}_\infty = \bar{Y}/A_\infty^{\frac{1}{2}}, \quad (7.30)$$

$$Q^{(\alpha)} = \frac{1}{A_\infty^{\frac{1}{2}}}\Omega_\alpha, \quad \alpha = \tfrac{5}{6}, \tfrac{4}{3}, \quad (7.31)$$

with $Q^{(\frac{5}{6})}$ and $Q^{(\frac{4}{3})}$ playing the roles of $Q^{(0)}$ and $Q^{(6)}$ of §5. We therefore give only the final results for the velocity and phase jumps, which are

$$\frac{\bar{U}A_\infty^{\frac{1}{2}} A'_\infty C^{(3)}}{\lambda} = 2\Theta'_\infty + \lambda x_2\left(\chi_3(+\infty) - \chi_3(-\infty)\right), \quad (7.32)$$

$$\lambda C^{(1)}\left(\bar{U}\Theta'_\infty + S_1 - \frac{\lambda x_2}{\bar{U}^2}\right) = 2A_\infty^{\frac{1}{2}} A'_\infty, \quad (7.33)$$

where $C^{(1)}$ and $C^{(3)}$ are given by (5.45) and (5.53), respectively.

7.3. *The amplitude and phase behaviour*

Equations (7.32) and (7.33) are easily solved for $A_\infty^{\frac{1}{2}} A'_\infty$ and Θ'_∞ to

$$A_\infty^{\frac{1}{2}} A'_\infty = -\tfrac{1}{3}\lambda a_\infty^{\frac{3}{2}}(S_1 + \lambda x_2 f(\bar{U})), \quad (7.34)$$

$$\Theta'_\infty = -\tfrac{1}{2}\theta'_\infty (S_1 + \lambda x_2 f(\bar{U})) + \frac{\lambda x_2}{\bar{U}}\left(f(\bar{U}) + \frac{1}{\bar{U}^2}\right), \quad (7.35)$$

where

$$f(\bar{U}) = \tfrac{1}{2}\bar{U}\left[2\left(\bar{U} + \frac{1}{\bar{U}} - \frac{1}{\bar{U}^3}\right) - \left(\bar{U} - \frac{1}{\bar{U}}\right)^2 \ln\left(\frac{\bar{U}+1}{\bar{U}-1}\right)\right], \quad (7.36)$$

and a_∞, θ'_∞, and D are given by (5.65)–(5.67). It is clear that A_∞ and Θ_∞ satisfy the upstream boundary conditions (7.3) and (7.4). In fact, the present solution is not too different from that of §5. The new effect comes from the linear terms in λx_2 which account for the mean-flow divergence.

7.4. *Interpretation of results*

Since λx_2 has a positive coefficient in (7.34) (cf. figure 7) while S_1 is negative, the mean-flow divergence effects eventually drive the growth rate to zero and ultimately cause the instability wave to decay. The present scaling will of course break down when the instability amplitude becomes too small, but there is little interest in carrying the solution beyond this point.

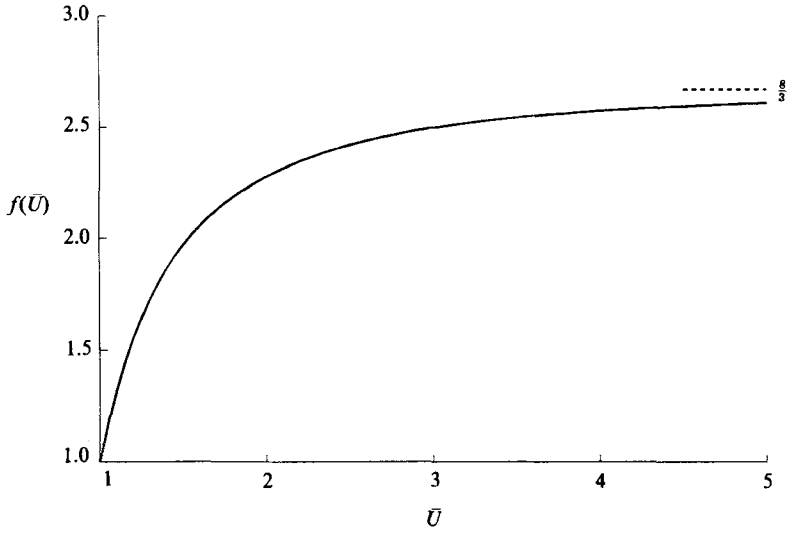

FIGURE 7. The function $f(\bar{U})$. The dashed line is the large-$\bar{U}$ asymptote $\frac{8}{3}$.

A calculation similar to the one used in obtaining (7.7) shows that the (actual) linear neutral state is determined by the dispersion relation

$$i\pi\left(\bar{U}k_{1N}-S_1+\frac{\lambda x_{2N}}{\bar{U}^2}\right)=\lambda x_{2N}(\chi_3(+\infty)-\chi_3(-\infty))-2k_{1N}, \tag{7.37}$$

where k_{1N} denotes the scaled (real) $O(\epsilon^{\frac{1}{3}})$-wavenumber perturbation at the neutral point due to the deviation from the hyperbolic-tangent profile (the neutral wavenumber is $1+\epsilon^{\frac{1}{3}}k_{1N}$) and x_{2N} denotes the scaled downstream distance (as measured from the non equilibrium nonlinear region) to that point. Equating real and imaginary parts in (7.37), using (7.10) and (7.36), and eliminating k_{1N}, we obtain

$$\lambda x_{2N}f(\bar{U})=-S_1, \tag{7.38}$$

which means that the nonlinear region approaches the neutral point as $|S_1|/\lambda\to 0$. Furthermore, (7.34) and (7.38) show that the neutral stability point (or point of maximum amplitude) is still equal to the linear neutral stability point, as has often been observed in experiments. It also follows from (7.34) that the maximum amplitude $\epsilon^{\frac{2}{3}}A_{\infty\max}$ is given by

$$\epsilon^{\frac{2}{3}}A_{\infty\max}=a_\infty\left(\frac{\epsilon S_1^2}{4f(\bar{U})}\right)^{\frac{2}{3}}. \tag{7.39}$$

The result (7.39) is independent of λ, which means that the maximum amplitude is independent of the viscosity.

The total critical-layer vorticity is given by minus

$$\Omega=1-\epsilon^{\frac{1}{3}}\lambda x_2/\bar{U}-\epsilon^{\frac{2}{3}}(\bar{Y}^2+2A_\infty\cos\bar{X}_\infty)+\epsilon^{\frac{5}{6}}\Omega_{\frac{5}{6}}+O(\epsilon). \tag{7.40}$$

Then, since all terms preceding $\Omega_{\frac{5}{6}}$ satisfy $\mathscr{L}_e\Omega_\alpha=0$, it follows from (7.22) that the critical-layer vorticity equation correct to, but not including, $O(\epsilon)$ terms, is

$$[\bar{Y}-\epsilon^{\frac{1}{6}}(\bar{U}\Theta'_\infty+S_1-2\lambda x_2c_1^{(0)})]\frac{\partial\Omega}{\partial\bar{X}_\infty}+A_\infty\sin\bar{X}_\infty\frac{\partial\Omega}{\partial\bar{Y}}=0. \tag{7.41}$$

It follows from (2.13), (2.14), and (2.33) that

$$U_{\mathrm{M}} = \bar{U} + \tanh\,(y + \epsilon^{\frac{1}{2}} 2\lambda x_2 c_1^{(0)}) + \epsilon^{\frac{1}{2}} 2\lambda x_2 G_0'(y) + O(\epsilon), \tag{7.42}$$

where $G_0(y)$ denotes $G(y)$ with $c_1^{(0)} = 0$. This shows that $\epsilon^{\frac{1}{2}} 2\lambda x_2 c_1^{(0)}$ can be interpreted as a displacement of the origin of the basic hyperbolic-tangent velocity profile. Thus, (7.41) explicitly shows that the critical layer is now shifted from the translated origin (i.e. the basic-flow inflexion point) by the amount $\epsilon^{\frac{1}{2}}(\bar{U}\Theta'_\infty + S_1)$ (compare this with (3.5)) and, consequently, that the slowly varying phase factor Θ'_∞ maintains the quasi-equilibrium state against changes in the mean flow. Finally, it is worth noting that, as in the linear case, the nonlinear amplitude and phase are independent of the streamline displacement $2\lambda x_2 c_1^{(0)}$ (see (7.34) and (7.35)).

8. Concluding remarks

By incorporating viscous effects into the nonlinear critical-layer analysis of I, we have succeeded in showing how an initially linear instability wave evolves as it propagates downstream. The development takes place first through a nonlinear non equilibrium critical layer, which gradually ages into a quasi-equilibrium critical layer (with variable cat's-eye vorticity). This, in turn, evolves into a final decaying stage, where the instability-wave growth rate is simultaneously affected by mean-flow divergence effects and (equilibrium) nonlinear critical-layer effects. The initial exponential growth of the linear instability wave is converted into algebraic growth in the nonlinear critical-layer region and this algebraic growth is ultimately converted into decay in the final stage of evolution. The nonlinear roll-up of the vorticity, which is so apparent in flow visualizations, occurs within the nonlinear critical-layer region of the present analysis.

Appendix. Elimination of Stewartson's singularity

(The variable cat's-eye vorticity issue)

Unlike the Benney & Bergeron (1969) solution, our result has variable vorticity in the closed-streamline region within the cat's-eye boundary. Benney & Bergeron (1969) evoked the Prandtl–Batchelor theorem to argue for constant vorticity but that result does not apply here because the rather rapid spatial development does not give viscosity time to fully act on the flow. Considerations similar to ours, probably led Stewartson (1981) to argue for constant vorticity in the related context of time-dependent Rossby-wave critical layers by noting that the solution to the Benney–Bergeron problem will exhibit a logarithmic singularity at the centre of the cat's-eye (see figure 1) unless the cat's-eye vorticity is taken to be constant.

While our problem has variable cat's-eye vorticity, the final solution turns out to be non-singular because the coefficient of c_0 in (5.30), which, as will be shown here, turns out to be a singular eigensolution, was eliminated using the generalized Prandtl–Batchelor theorem (5.11). We now show why Stewartson's (1981) argument cannot be used for this purpose.

To this end, we note that (5.25) and (5.26) show that

$$I \sim \tfrac{1}{2}\pi(\bar{\phi} + 2), \tag{A 1}$$

$$I_1 \sim -\tfrac{1}{2}\pi(\bar{\phi} + 2), \tag{A 2}$$

as $\bar{\phi} \to -2$. Hence, in view of (5.30), it follows that

$$F^{(0)} \sim \frac{2c_0}{\pi} \ln(\bar{\phi}+2) \quad \text{as} \quad \bar{\phi} \to -2. \tag{A 3}$$

This corresponds to the point $\bar{X} = \pi$ and $\bar{\eta} = 0$, i.e. the centre of the cat's-eye. However, both coefficients of the operator on the left-hand side of (5.5) go to zero there so that the viscous term on the right-hand side can no longer be treated as a higher-order term at the cat's-eye centre.

To obtain the appropriate equation for this region we introduce the new scaled inner variables

$$\tilde{X} = \left(\frac{a^{\frac{3}{2}}}{\bar{\lambda}}\right)^{\frac{1}{2}} (\bar{X} - \pi), \tag{A 4}$$

$$\tilde{\eta} = \left(\frac{a^{\frac{3}{2}}}{\bar{\lambda}}\right)^{\frac{1}{2}} \bar{\eta} \tag{A 5}$$

into (5.5) to obtain

$$\tilde{\eta} \frac{\partial \bar{Q}}{\partial \tilde{X}} = \tilde{X} \frac{\partial \bar{Q}}{\partial \tilde{\eta}} + \frac{\partial^2 \bar{Q}}{\partial \tilde{\eta}^2}, \tag{A 6}$$

to lowest order of approximation. Matching the solution with (A 3) leads to the boundary condition

$$\bar{Q} \sim \frac{2c_0}{\pi} \ln(\tilde{X}^2 + \tilde{\eta}^2) \quad \text{as} \quad \tilde{X}^2 + \tilde{\eta}^2 \to \infty, \tag{A 7}$$

which follows immediately from (5.8), (A 4), and (A 5). The only other requirement is that the solution remain bounded and have continuous derivatives for all $\tilde{X}$ and $\tilde{\eta}$.

Since (A 6) is clearly parabolic, it might at first glance seem rather strange that its solution be required to satisfy a boundary condition of the type (A 7) that is imposed all around an outer boundary. But since the coefficient of the first derivative with respect to $\tilde{X}$ changes sign, (A 6) is of the actually of the singular parabolic type (Stewartson 1951) and its solution can be expected to exhibit elliptic behaviour.

We, therefore, borrow a technique from the theory of elliptic partial differential equations and introduce the complex variables

$$Z = \tilde{X} + \mathrm{i}\tilde{\eta}, \tag{A 8}$$

$$Z^* = \tilde{X} - \mathrm{i}\tilde{\eta}, \tag{A 9}$$

as new independent variables to obtain

$$\left(\frac{\partial^2}{\partial Z^2} + \frac{\partial^2}{\partial Z^{*2}} - 2\frac{\partial^2}{\partial Z \partial Z^*} - \mathrm{i}Z\frac{\partial}{\partial Z} + \mathrm{i}Z^*\frac{\partial}{\partial Z^*}\right)\bar{Q} = 0. \tag{A 10}$$

Then since $\bar{Q}$ must be real, we seek a solution of the form

$$\bar{Q} = F(Z) + [F(Z)]^*, \tag{A 11}$$

where the asterisk denotes complex conjugation. It follows that F must satisfy

$$\frac{\mathrm{d}^2 F}{\mathrm{d}Z^2} - \mathrm{i}Z\frac{\mathrm{d}F}{\mathrm{d}Z} = \mathrm{i}C, \tag{A 12}$$

where C is a real constant, since $[F(Z)]^*$ is only a function of Z^*.

This equation is easily integrated to obtain.

$$F = C(\tfrac{1}{2}\pi\mathrm{i})^{\frac{1}{2}} \int^{Z} w\left(\frac{Z}{(2\mathrm{i})^{\frac{1}{2}}}\right) \mathrm{d}Z. \tag{A 13}$$

where w denotes the scaled complex error function $w(z) = \mathrm{e}^{-z^2}\,\mathrm{erfc}\,(-\mathrm{i}z)$, defined on p. 297 of Abramowitz & Stegun (1964). Using the asymptotic expansion 7.1.23 on p. 298 of Abramowitz & Stegun (1964), we find that

$$F \sim -C\left(\ln Z - \sum_{m=1}^{\infty} \frac{\mathrm{i}^m\, 1\times 3\times \ldots \times (2m-1)}{2mZ^{2m}}\right) \quad \text{as} \quad Z \to \infty. \tag{A 14}$$

$\bar{Q}$ will, therefore, satisfy the matching condition (A 5) if

$$C = -\frac{2c_0}{\pi}. \tag{A 15}$$

Finally, $\bar{Q}$ remains bounded and has continuous derivatives of all orders, because w is an entire function of Z as can be seen from 7.1.8, p. 297 of Abramowitz & Stegun (1964). This shows that Stewartson's singularity can be removed and that this 'singular' eigensolution cannot be precluded just because of its logarithmic behaviour at the centre of the cat's eye.

REFERENCES

Abramowitz, M. & Stegun, I. A. 1964 *Handbook of Mathematical Functions.* US National Bureau of Standards.

Batchelor, G. K. 1956 On steady laminar flow with closed streamlines at large Reynolds number. *J. Fluid Mech.* **1**, 177–190.

Bénney, D. J. & Bergeron, R. F. 1969 A new class of non-linear waves in parallel flows. *Stud. Appl. Maths.* **48**, 181–204.

Bodonyi, R. J., Smith, F. T. & Gajjar, J. 1983 Amplitude-dependent stability of boundary-layer flow with a strongly nonlinear critical layer. *IMA J. Appl. Maths.* **30**, 1–19.

Brown, S. N. & Stewartson, K. 1978 The evolution of the critical layer of a Rossby wave II. *Geophys. Astrophys. Fluid Dyn.* **10**, 1–24.

Gajjar, J. & Smith, F. T. 1985 On the global instability of free disturbances with a time-dependent nonlinear viscous critical layer. *J. Fluid Mech.* **157**, 53–77.

Goldstein, M. E. & Durbin, P. A. 1986 Nonlinear critical layers eliminate the upper branch of spatially growing Tollmien–Schlichting waves. *Phys. Fluids* **29**, 2344–2345.

Goldstein, M. E., Durbin, P. A. & Leib, S. J. 1987 Roll-up of vorticity in adverse-pressure-gradient boundary layers. *J. Fluid Mech.* **183**, 325–342.

Goldstein, M. E. & Leib, S. J. 1988 Nonlinear roll-up of externally excited free shear layers. *J. Fluid Mech.* **191**, 481–515.

Haberman, R. 1972 Critical layers in parallel flows. *Stud. Appl. Maths.* **51**, 139–161.

Haynes, P. H. 1985 Nonlinear instability of a Rossby-Wave critical layer. *J. Fluid Mech.* **161**, 493–511.

Huerre, P. & Scott, J. F. 1980 Effects of critical layer structure on the nonlinear evolution of waves in free shear layers. *Proc. R. Soc. London* A **371**, 509–524.

Smith, F. T. & Bodonyi, R. J. 1982 Nonlinear critical layers and their development in streaming-flow stability. *J. Fluid Mech.* **118**, 165–185.

Stewartson, K. 1951 On the impulsive motion of a flat plate in a viscous fluid. *Q. J. Appl. Maths.* **4**, 182–198.

Stewartson, K. 1978 The evolution of the critical layer of a Rossby wave. *Geophys Astrophys. Fluid Dyn.* **9**, 185–200.

Stewartson, K. 1981 Marginally stable inviscid flows with critical layers. *IMA J. Appl. Maths.* **27**, 133–175.

Warn, T. & Warn, H. 1978 The evolution of a nonlinear critical level. *Stud. Appl. Maths.* **59**, 37–71.